1-1-2019

Evaluation of wireless router antennas and 3d-printed simulated antenna designs

Bibek Kattel

EVALUATION OF WIRELESS ROUTER ANTENNAS AND 3D-PRINTED SIMULATED ANTENNA DESIGNS

A Thesis

Presented for the

Master of Engineering Science in Electrical Engineering

Degree

The University of Mississippi

Bibek Kattel

August 2019

ABSTRACT

As the size of the electronics devices is decreasing, the overall size of the antenna inside them is also decreasing. As the antenna size becomes smaller, it is more difficult to manufacture them with the process of traditional manufacturing that uses the subtractive method to manufacture a structure. This is where additive manufacturing has an edge on traditional manufacturing. The use of this method to manufacture antennas has been discussed in this thesis. Five antennas from a wireless router are evaluated by modeling them in CST Microwave Studio and are modified so that they can be manufactured with 3D printing. The overall difficulties of manufacturing antennas using 3D printing have been discussed and a few solutions have been proposed to tackle those difficulties. The modified antennas were simulated in CST Microwave Studio and the performance of the antennas before and after modification is compared to make sure that the performance of the modified antennas is similar to that of the original physical antennas used in the wireless router.

ACKNOWLEDGMENTS

I want to thank my committee members Dr. Elliot Hutchcraft, Dr. Richard Gordon, and Dr. Ellen Lackey for taking the time to review my thesis. My advisors Dr. Hutchcraft and Dr. Gordon have been an invaluable source of guidance and inspiration in my search for new questions. I am equally thankful to all the professors and staffs of the Electrical Engineering department for the support throughout my studies. I also want to extend my gratitude to my friends, families who always have been an unceasing source of motivation for me. Last but not the least I am grateful to the Nepalese Students Association at Ole Miss (NEPSA) family for always being a home away from home during my stay here at the University of Mississippi.

TABLE OF CONTENTS

LIST OF FIGURES

CHAPTER I

INTRODUCTION

An antenna is a transducer that converts radio-frequency fields into alternating current and vice versa. An antenna is an integral part of all modern communication systems as it is finding more and more usefulness in a lot of modern devices like cellphones, smart home devices, modern medical technologies, and others. The complexity of electronic devices is increasing while the devices themselves are shrinking in size. The overall reduction in the size of the devices has also led to a reduction in the physical dimension of an antenna. As an antenna size is becoming smaller, it is becoming more difficult to manufacture complex miniature antenna structures by the process of traditional manufacturing.

This is where the use of 3D printing to manufacture such miniature structures finds its usefulness. One of the best advantages that this process offers over traditional manufacturing is the fabrication of miniature antenna structures with very accurate dimensions. This technology also enables scientists and engineers all around the world to experiment with various kinds of shapes and structures as well as materials that can be used to design and test novel antennas. An antenna prototype designed in an antenna simulation software like CST Microwave Studio can be essentially translated into its physical counterpart within minutes with 3D printing facilities. The 3D printing facilities that have gained a widespread use nowadays are able to dispense two different types of materials, which makes it extremely convenient to manufacture both the

conducting and the dielectric layers of an antenna simultaneously. While it is a moot question to argue whether 3D printing will replace the traditional antenna manufacturing systems in large scale manufacturing, nonetheless, we can conclude that 3D printing is an upcoming technology which knows no bounds in innovation and convenience to develop new antenna structures.

INTRODUCTION TO 3D PRINTING

3D printing or additive manufacturing is a process of making a solid 3-dimensional structure from a digital 3D model, the machine that can accomplish this task is called a 3D printer. A 3D printer builds shapes by adding successive layers of material over the previous layer step by step. We can visualize each of these layers as a thinly sliced horizontal cross-section of the eventual object to be manufactured. More complex shapes can be easily manufactured using this method than by traditional manufacturing. 3D printing provides endless opportunities for the fabrication of a wide range of different EM structures with integrated conductor and dielectric material along with addressing the alignment difficulties that occur in the conventional manufacturing process [1].

The first step for 3D printing is designing a digital 3D model. This is generally done through computer-aided design. In our case, the antenna that was modeled and simulated in CST Microwave Studio also serves as the 3D model that can be used for 3D printing. The next step is called slicing, which is dividing a 3D model into hundreds or thousands of horizontal layers with slicing software. A 3D model needs to be sliced to make it 3D printable because the 3D printing works by adding a new layer on top of the existing layer, and slicing defines each layer to be printed one at a time. The sliced model is fed to the 3D printer which then prints the model with a

physical material one slice at a time. Depending upon the purpose, the physical material used during the printing may be plastic, molten metal, dielectric material, and others [2].

The 3D printing technology started with molten plastic as the printing material, but different types of metal and their alloys are being used more and more nowadays as the technology is advancing. 3D printing is gaining wide uses in different disciplines including electrical engineering thanks to the features like rapid prototyping and rapid manufacturing, reasonable accuracy, fully 3-D topologies, and low fabrication cost [3].

BRIEF OVERVIEW OF PREVIOUS WORK

Antenna design using 3D printing is gaining a lot of popularity nowadays as we see more and more ongoing research and development in this area. 3D printing of microwave components is attractive as the dimensions of antennas, waveguides, and other components are significantly large, and existing technologies with printing resolution below 25μm can be used [4]. Affordable 3D printing of a patch antenna, a logo-based patch, a folded E-patch, and a wideband bilateral Vivaldi antenna has been discussed in [4]. Also, the manufacturing of many microwave components including waveguides, horn antennas, and directional couplers have been demonstrated using 3D printing in [5,6]. A planar bowtie antenna has been constructed in [7]. We can see that even though 3D printing is already popular in antenna design, more planar antennas have been designed with this method than 3-dimensional antenna structures. Also, there are very few antenna designs that have included a dielectric material in their antenna design. This can be attributed to the fact that the dielectric material causes an unprecedented change in the resonating frequency as well as the return loss at the resonating frequency. So, in this research, our objective

is to use the 3D printing to design a 3D antenna structure filled with a dielectric material, preserving the antenna's performance characteristics as well as its basic design structure.

RESEARCH OBJECTIVES

The objective of this research is to study the performance of wireless router antennas and modify them in such a way that they can be manufactured by the method of additive manufacturing. The research is divided into two main sections as listed below:

1. Modeling of the physical antennas in CST Microwave Studio
2. Modifying the antennas by filling the antennas with a dielectric substrate while retaining the performance characteristic of the original router antennas. A dielectric material with relative permittivity 2.45 has been taken for antenna designs.

CHAPTER II

BACKGROUND THEORY

In this thesis, we have taken an Extreme Wireless Router that has five different Wi-Fi and Bluetooth antenna existing in mutual co-existence. Out of the five antennas, three of them are bowtie antennas, one is a winged antenna and another one is an inverted antenna. The wireless router is shown in Figure 1. We can see that apart from the antenna structure, the five antennas can also be distinguished with the colors of the feeding wire, which are green, blue, black, red, and white. These antennas are described in the advancing sections of this chapter.

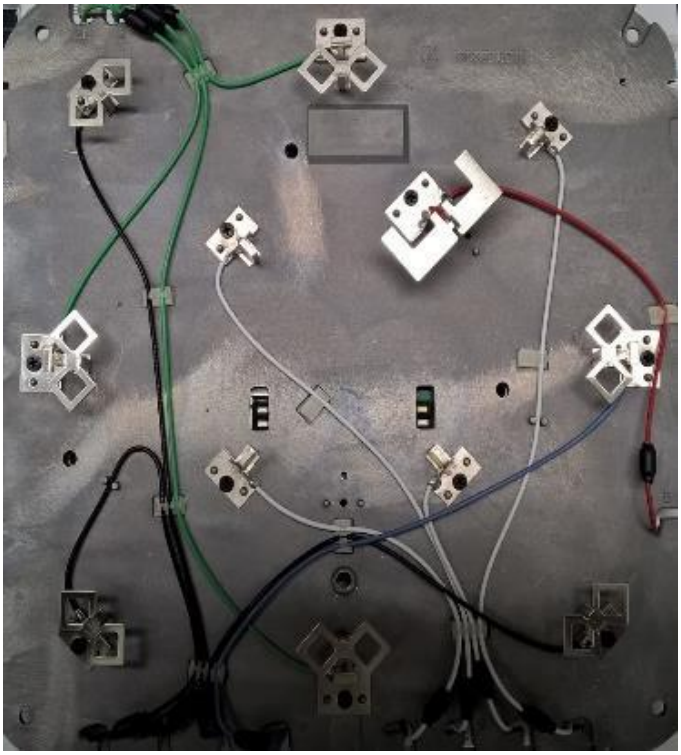

Figure 1. Antennas in the Extreme Wireless Router

BOWTIE ANTENNAS

A bowtie antenna is a type of biconical antenna which has two metal pieces arranged in the configuration resembling a bowtie. The antenna feed is at the center of the antenna. Theoretically, such antennas have infinite bandwidth because they work almost at any frequency as the antenna looks the same for all frequencies. These antennas have a similar radiation pattern to dipole antennas. A typical bowtie antenna structure is shown in figure 2.

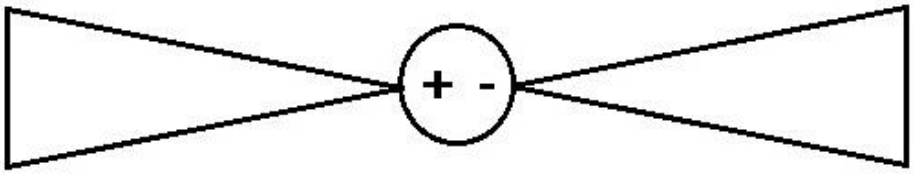

Figure 2. A Typical Bowtie Antenna

Out of five antennas in the wireless router, there are three bowties antennas. Unlike a planar bowtie shown in figure 2, the bowties in the router are modified bowtie antennas in 3-dimensional structures specifically intended to operate in the 2.4 GHz Wi-Fi, Bluetooth and in the 5GHz Wi-Fi frequency. The three bowties seem to have the same dimensions, and hence they were all expected to have quite similar performance. The primary difference between these antennas was the way they were fed, which was not expected to make a drastic difference in performance. In the wireless router, the blue and black wired bowties are tied to 2.4 GHz Wi-Fi radio while the green wired bowtie is tied to the dual-band, dedicated network sensor radio (both 2.4 GHz and 5 GHz Wi-Fi). Figure 3-5 shows the blue, black and the green wired bowtie antenna respectively.

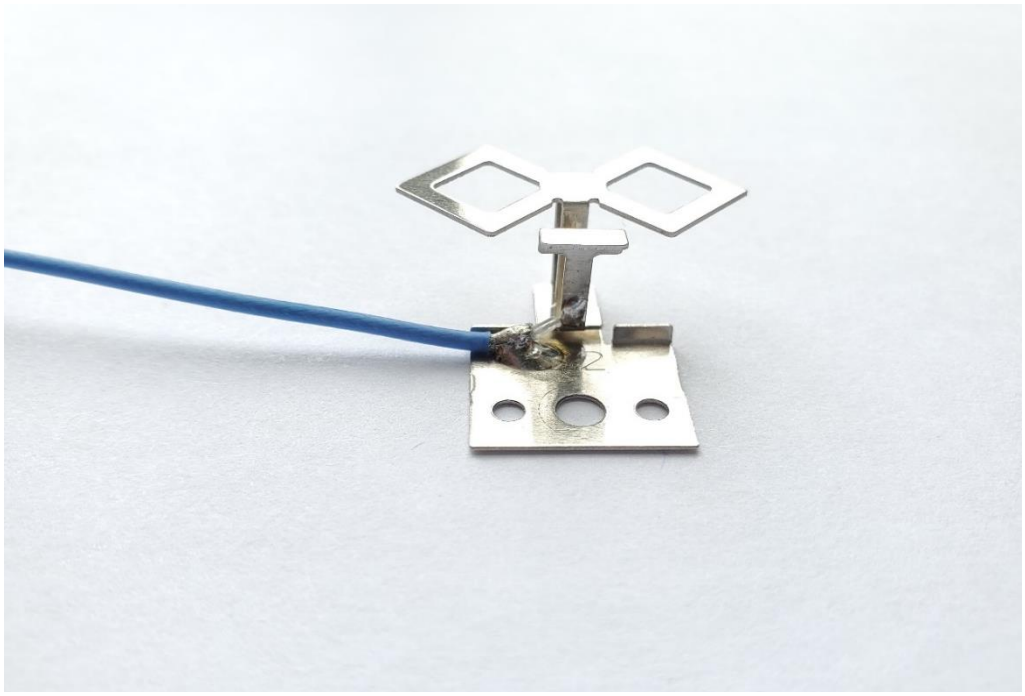

Figure 3. Blue Wired Bowtie Antenna

Figure 4. Black Wired Bowtie Antenna

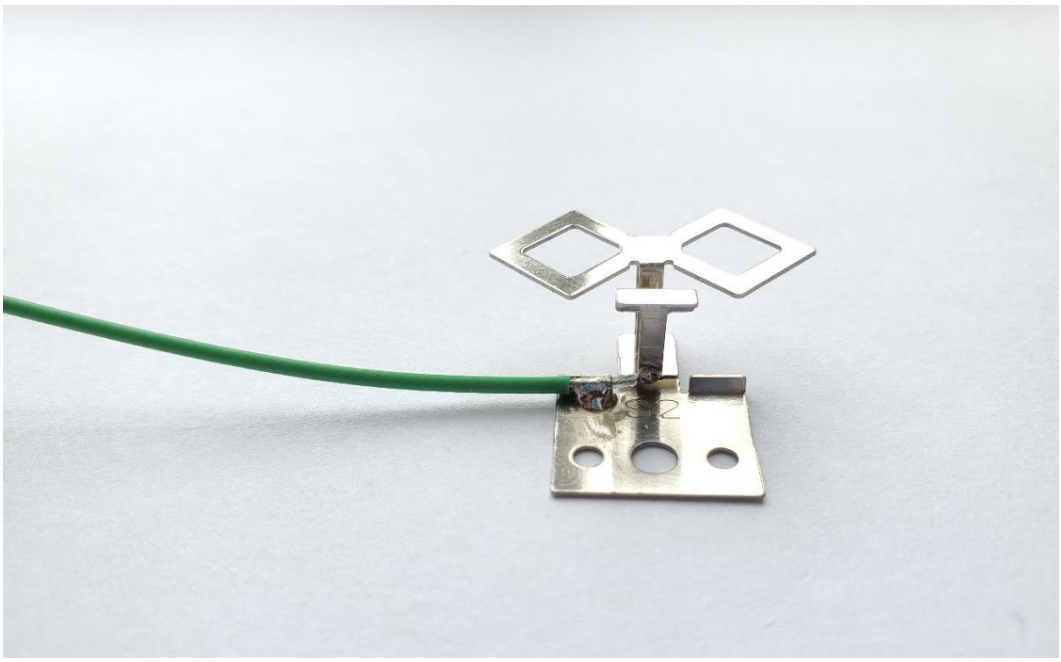

Figure 5. Green Wired Bowtie Antenna

WINGED ANTENNA

A winged antenna is a type of modified dipole antenna. The dipole arms are modified to resemble the shape of a wing and hence the name. The wireless router has one winged antenna. This winged antenna is fed to each side of the wing and since the feeding wire of the winged antenna is of red color, it is also referred to as the red wired antenna in this thesis. In the wireless router, this antenna is used for Bluetooth Low Energy radio and is operated in the 2.4 GHz band. The antenna is shown in figure 6.

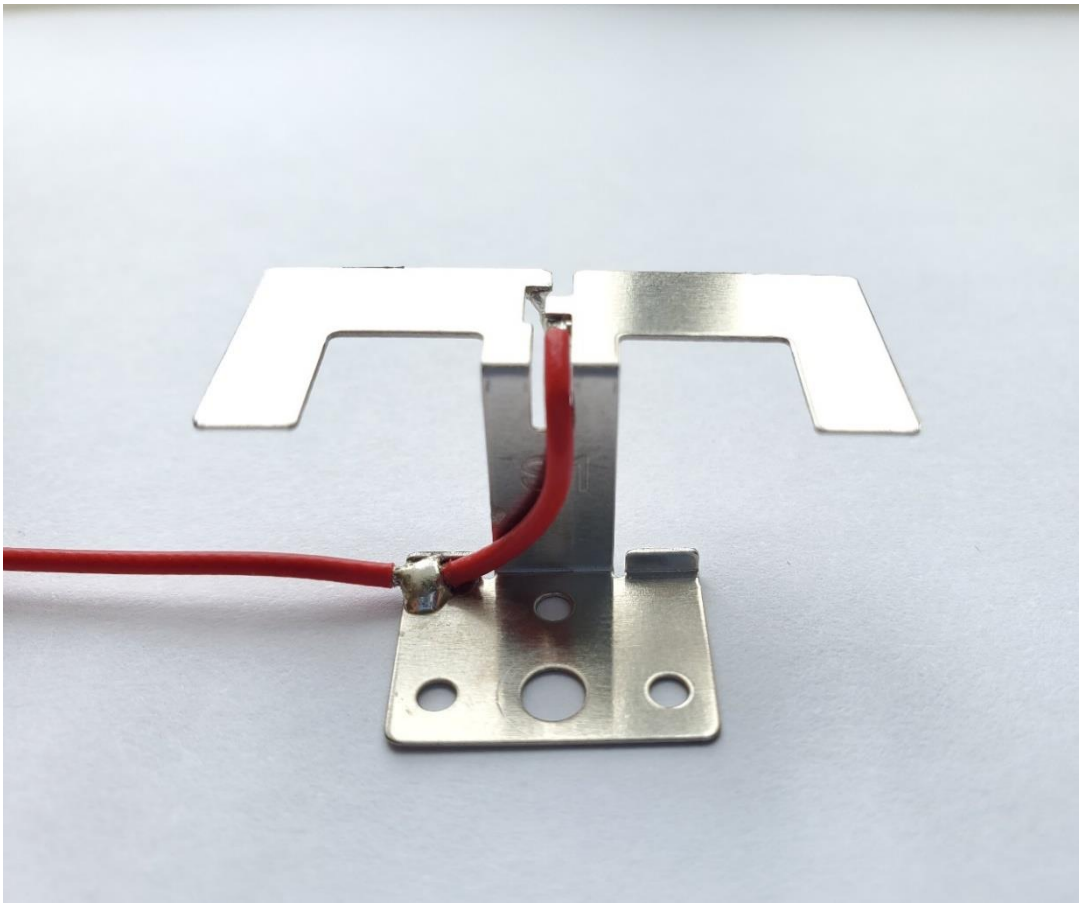

Figure 6. Red Wired Winged Antenna

INVERTED ANTENNA

The inverted antenna has the characteristics of small size, lightweight, low profile, low manufacturing cost and easy integration with the portable terminals and can be referred to as a preferable candidate for WLAN applications. An inverted antenna mostly consists of the following parts: a radiating patch, a shorting strip, a feeding part, and a system ground plane [8]. In the wireless router, the inverted antenna has been used for 5 GHz Wi-Fi radio. The inverted antenna which is also called as white wired antenna in this thesis is shown in figure 7.

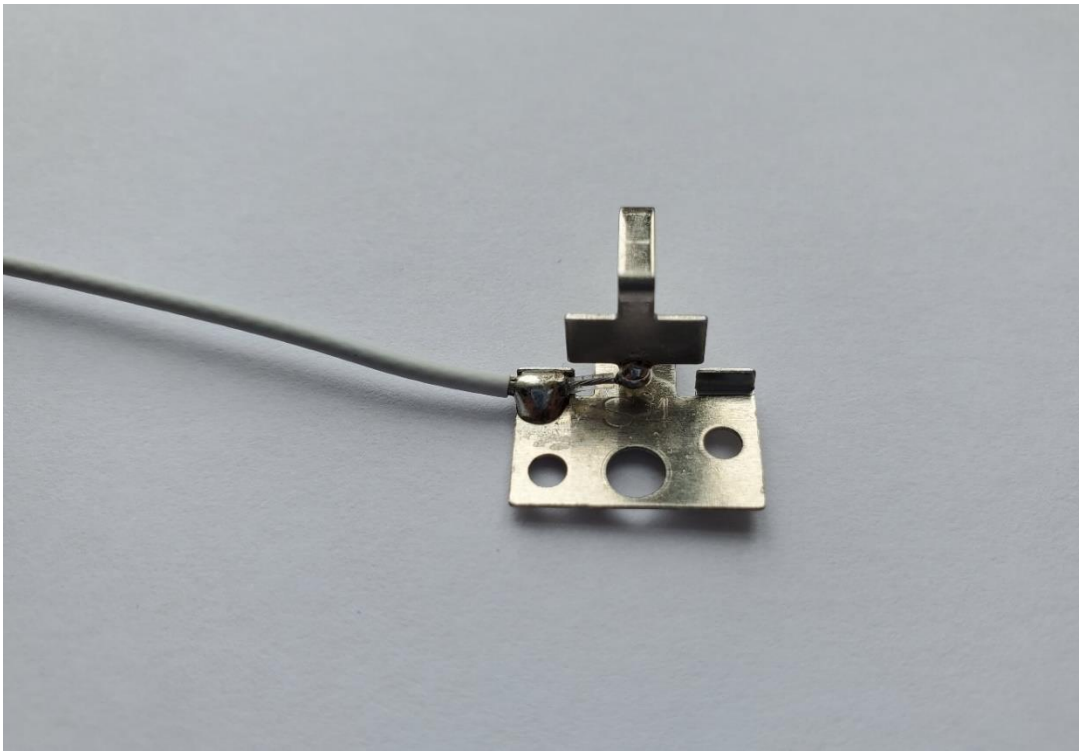

Figure 7. White Wired Inverted antenna

ANTENNA MEASUREMENTS

An antenna is characterized by a number of performance measures which has to be taken under consideration while selecting or designing an antenna for a particular application. Antenna measurement techniques refer to the testing/measurement of antennas to ensure that the antenna meets the required specifications. In this thesis, we are focusing on the two of the most important antenna measurements namely, S-parameters or return loss measurements and the radiation pattern measurements of an antenna. These antenna measurements help us to identify the performance characteristics of an antenna.

S PARAMETERS

Scattering parameters or commonly known as S-parameters describe the input-output relationship between ports (or terminals) in an electrical system. For instance, if we have 2 ports that are called Port 1 and Port 2, then S_{12} represents the power transferred from Port 2 to Port 1. Likewise, S_{21} represents the power transferred from Port 1 to Port 2. In practice, the most commonly quoted parameter in regards to antennas is S_{11}. The measure of S_{11} represents how much voltage is reflected from the antenna, and hence S_{11} is known as the reflection coefficient or return loss.

If S_{11}=0 dB, then all the wave is reflected from the antenna and nothing is radiated. If S_{11}= -10 dB, this implies that if 3 dB of power is delivered to the antenna, -7 dB is the reflected power. The remainder of the power was "accepted by" or delivered to the antenna. This accepted power is either radiated or absorbed as losses within the antenna. While designing an antenna we want the return loss to be as low as possible so that the majority of the power delivered to the antenna is radiated [9].

The reflection coefficient (denoted by Γ) is defined as the ratio of voltage reflected by the antenna to the total incident voltage. Mathematically,

$$\Gamma = \frac{\text{total reflected voltage by the antenna}}{\text{total incident voltage}}$$

Then the return loss (denoted by S_{11}) is given by :

$$S_{11} = 20 \log |\Gamma|$$

Since the reflected voltage is generally less than the total incident voltage, the value of the reflection coefficient is a positive number less than 1. And the logarithm of such a value is negative. So, the return loss is a negative value in decibels (dB). For a good antenna, the return loss (S_{11}) is expected to be less than -10 dB over the useful frequency ranges of the antenna.

RADIATION PATTERN

A radiation pattern of an antenna gives the variation of the power radiated by an antenna as a function of the angle and direction from the antenna. Basically, it shows how much power an antenna radiates over a particular direction at a particular distance. In this thesis, since the radiation pattern was taken at the far field region of an antenna, it is also referred to as far field pattern. The radiation pattern depends on the type of the antenna. The radiation pattern of an isotropic antenna is a sphere meaning that it radiates equally over the surface of the sphere.

Some antennas may also be described as "omnidirectional", which for an actual antenna means that the radiation pattern is isotropic in a single plane. Examples of omnidirectional antennas include the dipole antenna and the slot antenna.

Another type of antenna is the directional antenna in which the antenna radiates most of the power in a particular direction. The radiation pattern of such antennas is also directed toward the direction in which most of the power is radiated.

Figure 8 shows the radiation pattern of CST modeled red wired antenna where we can see that the maximum power is radiated towards the z-axis classifying it as a directional antenna.

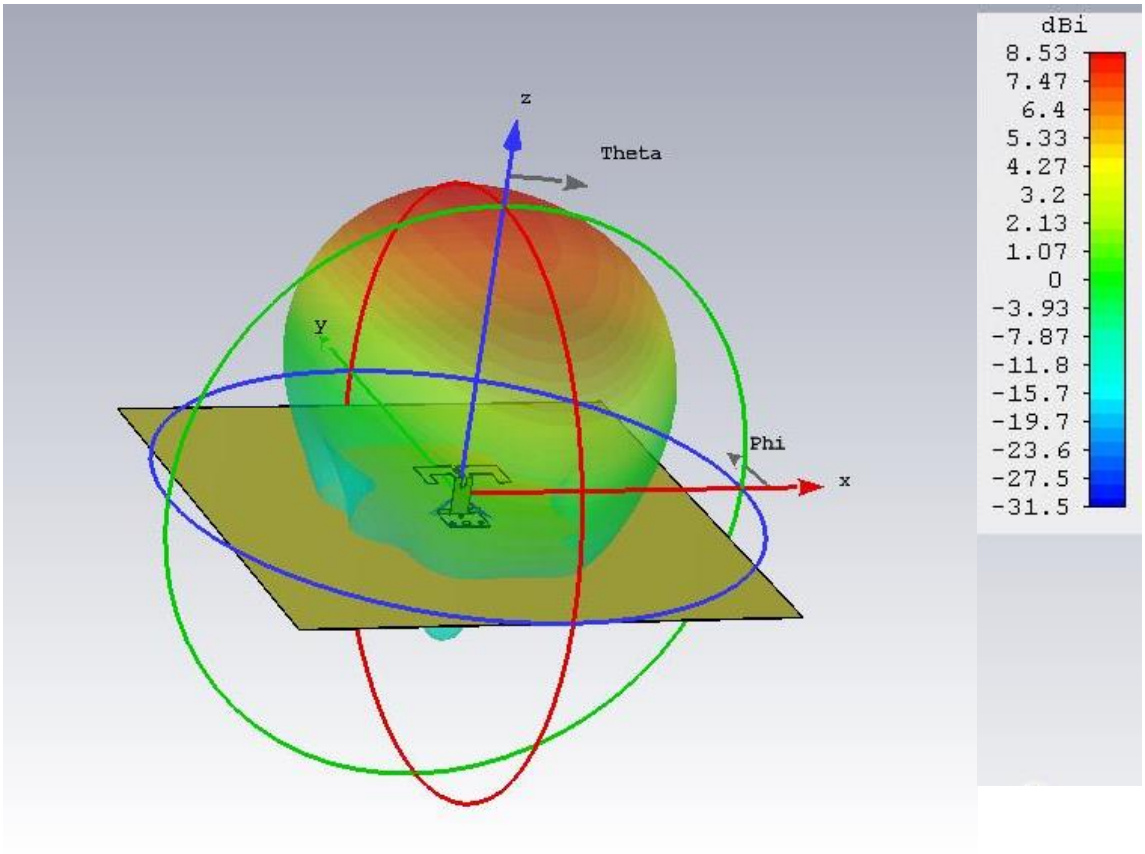

Figure 8. Radiation Pattern Plot for CST Modeled Red Wired Antenna with Ground Plane at 2.756 GHz

CHAPTER III

EXPERIMENTAL VERIFICATION AND DESIGN PROCEDURE

The experiment to manufacture these five antennas using the 3D printing process all began with the modeling of these five physical antennas in CST Microwave Studio. CST Microwave Studio is a specialist tool for the 3D electromagnetic simulation of high-frequency components [10]. This software was selected upon the basis of availability of license in the university's computers as well as its widespread use by scientists and engineers, due to which an ample number of tutorials and troubleshooting guides are available on the web. All of the above five antennas were modeled in CST and reverse engineered to optimize them for 3D printing so that they still have ideally the same characteristics as the original antennas. To begin with, we measured the return loss and radiation pattern of the physical antennas using a network analyzer.

ANTENNA MEASUREMENTS INSIDE THE ANECHOIC CHAMBER

Basically, when we want to measure an antenna, the most common and desired measurements include an antenna's radiation pattern, antenna gain and efficiency, the return loss, and therefore the VSWR, the bandwidth, and the polarization [9]. When we want to focus on the performance of the antenna, a good measure of antenna performance is the return loss of the antenna. For a good antenna, the return loss is expected to be well below (less than) -10 dB over the respective useful frequency ranges of the antenna. If that is true, then the antenna would be

considered to operating effectively for that particular frequency band. It was expected that resonances at harmonic frequencies might be present, so the return losses for all of the antennas were measured by sweeping frequency from 500 MHz – 12.5 GHz. Each of the five antennas under test (AUT) was measured separately by mounting them on a ground plane so that we could determine each antenna's individual performance. The ground plane was put in place to mimic the ground plane in the wireless router itself. The setup used for the radiation pattern measurements is shown in Figure 9 below [11].

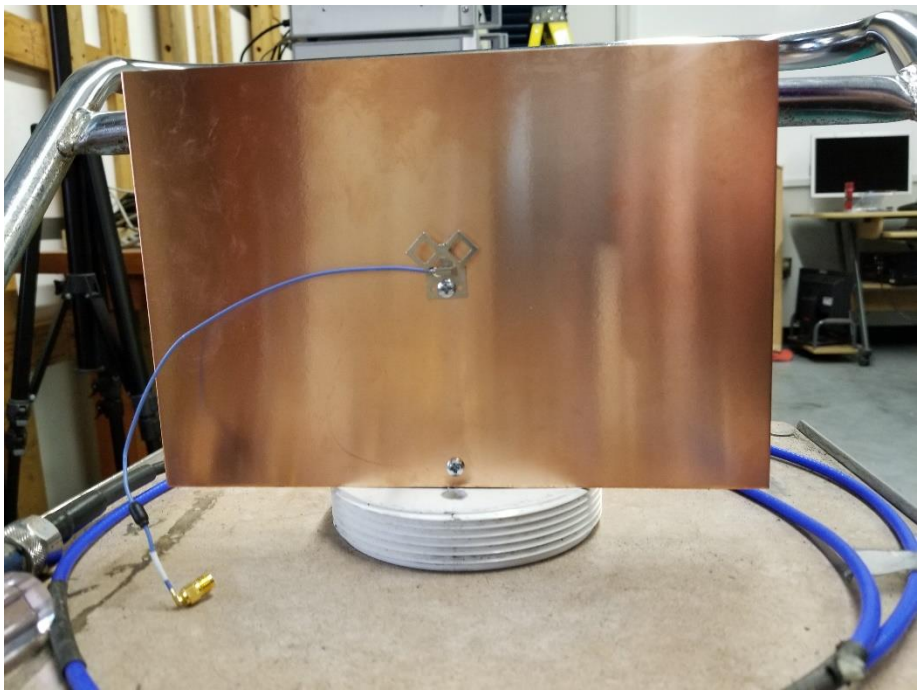

Figure 9. Antenna Measurement Apparatus

The return losses of the antennas were measured with a network analyzer, and the results were exported into a digital text file. This file was later imported to Python programming language

for further processing.

ANTENNA REMODELING IN CST

To simulate the antennas in CST Microwave Studio it is necessary for us to design an identical 3-dimension antenna model as the original physical antenna. We started with the measurement of each of the dimensions for the antennas with digital Vernier calipers. The

Figure 10. Vernier Calipers Used to Take Physical Antenna Dimensions

measured antenna dimensions were used to create a corresponding digital model in CST Microwave Studio. We wanted the digital model to have an identical structure and each measurement as precise as possible compared to the physical antennas. After this, the feed point in the physical antennas was recognized and efforts were made so that close to the same point was used for feeding the CST model. The actual physical measurement conditions were also considered

and the model designed in CST Microwave Studio was simulated under the same conditions. We were also careful about the frequencies at which far field pattern of the physical antennas was measured and hence the same frequency was set in the CST Microwave Studio to observe a far-field pattern in those particular frequencies. The input impedance was set to 50 Ohm and the time domain solver in CST was used to solve for the return loss and far-field patterns of the antennas. The obtained results for return loss and the radiation patterns were exported to an ASCII text file. These files were then imported into Python programming language to draw the plots of both the CST result and the physical antenna measurement result in the same figure. In particular, we analyzed two plots to compare the two sets of results: the S_{11} plot and the radiation pattern plot. A discussion of the results follows the following plots:

S_{11} PLOTS: MEASURED VS CST SIMULATED

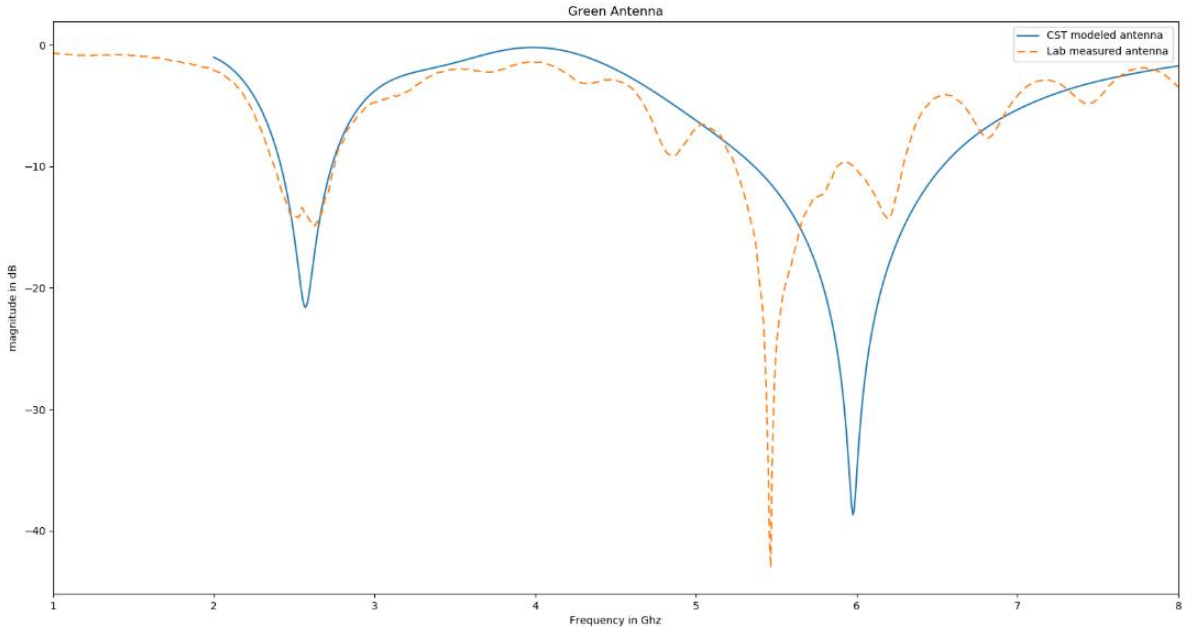

Figure 11. S_{11} for Green Wired Antenna: Measured Vs. CST Simulated Antenna

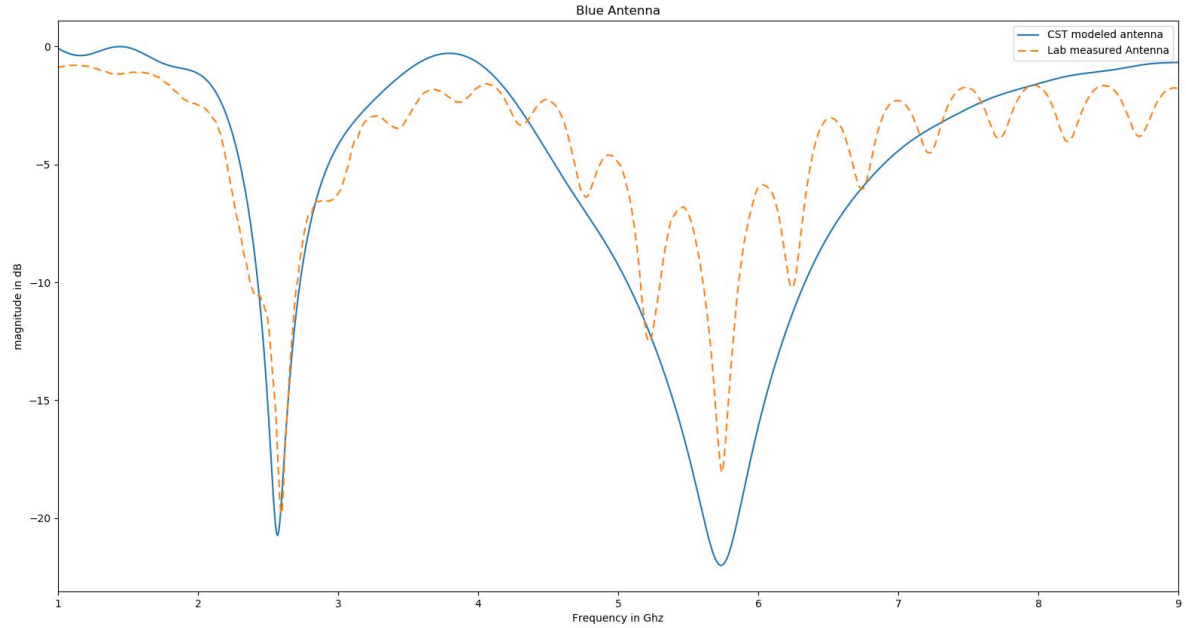

Figure 12. S_{11} for Blue Wired Antenna: Measured Vs. CST Simulated Antenna

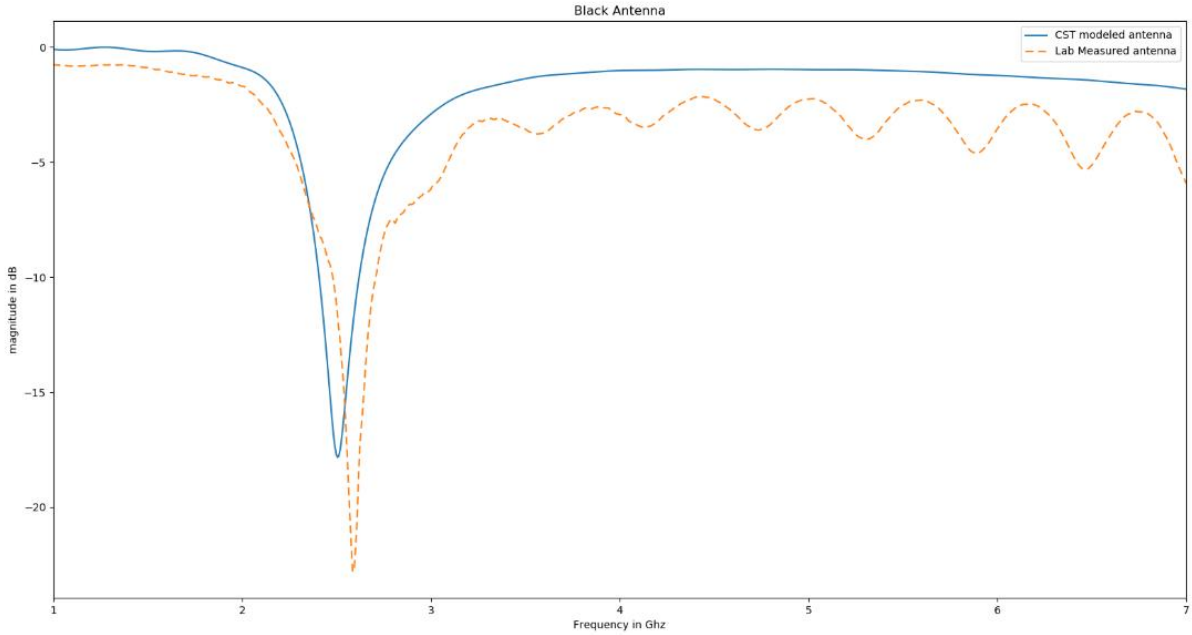

Figure 13. S_{11} for Black Wired Antenna: Measured Vs. CST Simulated Antenna

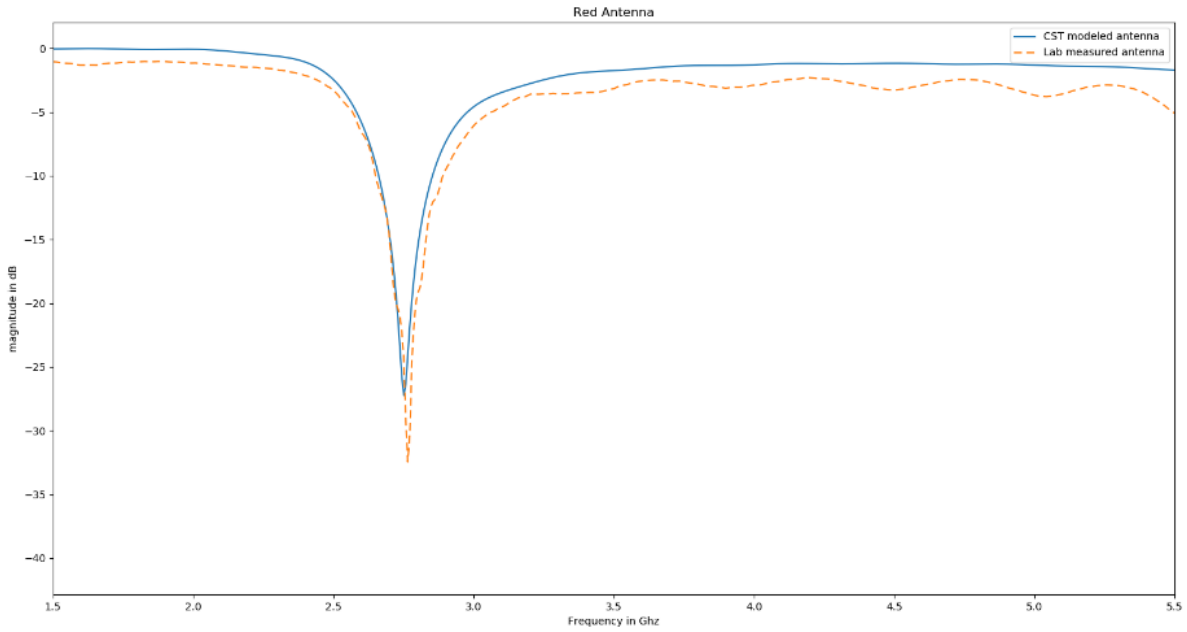

Figure 14. S_{11} for Red Wired Antenna: Measured Vs. CST Simulated Antenna

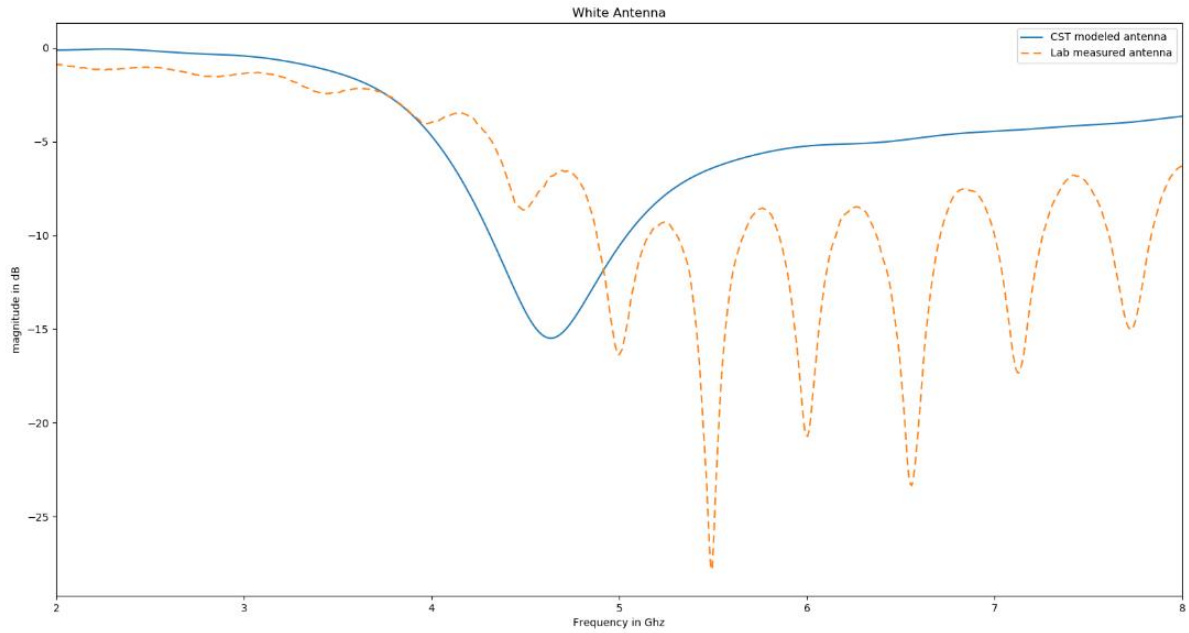

Figure 15. S_{11} for White Wired Antenna: Measured Vs. CST Simulated Antenna

As seen from the above plots (figure 11-15) for the return loss (S_{11}) we can say that the results for CST designed antennas are similar in comparison with the actual physical antennas. In the above plots, the blue curve represents the CST modeled antenna result while the dashed orange curve represents results for the physical antenna measurements. On the basis of the above plots, the performance comparison for the CST modeled antenna and the physical antenna can be summarized as below:

Figure 11 shows the CST modeled antenna result and physical measurement antenna result for the green wired bowtie antenna. As seen from the figure, the green wired bowtie antenna resonates at both Wi-Fi bands. The green wired antenna is connected to the radio that is used for determining network congestion (for both Wi-Fi bands), so it is necessary for it to operate efficiently in both Wi-Fi bands, and it indeed does. The bandwidth at the 5GHz range is wider, and the resonance is also quite deeper compared to the 2.4 GHz range. It is interesting to note that for both sets of data the resonant frequency in lower Wi-Fi range coincide which is about 2.6 GHz but it differs in the upper Wi-Fi band which is about 5.756 and 6 GHz for the physical measurement result and CST simulated measurement result respectively. The error during the dimension measurement with Vernier calipers must be the cause for such discrepancy. This error caused the dimension of the CST modeled antenna to differ from that of the physical antennas. Since the wavelength of the lower frequency is large in comparison to the higher frequency, the lower frequency is less prone to such errors. That is why we can see a deviation in the deepest resonance frequency in the upper Wi-Fi band but not on the lower W-Fi band. However, we are not much concerned in rectifying this error now because in the second part of the thesis we will modify this antenna to make it resonate at any two desired frequencies in the lower and upper Wi-Fi band.

Figure 12 shows the CST modeled antenna result and physical measurement antenna result for the blue wired bowtie antenna. Physically, the blue wired bowtie is almost similar to the green wired bowtie, and the feed points are also identical, and unsurprisingly it shows similar performance characteristics as the green wired bowtie antenna. This time the physical antenna measurement result, as well as the CST simulated result, almost show the same resonant frequency for both the Wi-Fi bands indicating that we have negligible measurement error. This antenna resonates around at 2.6 GHz and 5.756 GHz, for the lower and upper Wi-Fi band respectively. One thing to note is that, even though this antenna resonances at both bands, the antenna is only connected to the 2.4 GHz Wi-Fi radio.

Figure 13 shows the CST modeled antenna result and physical measurement antenna result for the black wired bowtie antenna which shows that the antenna resonates only at the 2.4 GHz Wi-Fi band. While the black wired bowtie antenna has an equivalent bowtie structure compared with the green and blue wired bowtie antennas, it differs in the feeding structure. And this different feeding structure is likely the reason it resonates at the 2.4 GHz band but not on the 5 GHz band. The feeding structure seems to suppress the 5 GHz band. In the case of this black wired antenna, both the physical antenna and the CST simulated antenna seem to resonate at around 2.5 GHz. It is connected to a 2.4 GHz radio Wi-Fi, and the performance results show it as a good radiator in the band.

Figure 14 shows the CST modeled antenna result and physical measurement antenna result for the red wired winged antenna which is used for the BLE radio in the wireless router. It has a resonance in the BLE band (which is also similar to the frequency range of the 2.4 GHz Wi-Fi band) near 2.756 GHz, and during the physical antenna measurements, it was seen that it also

resonates near the upper end of the 5 GHz Wi-Fi band at 5.984 GHz as well as in the upper-frequency ranges. But, since it is only used for a 2.4 GHz application, it is expected that the radio will incorporate a filter to filter out other bands except for the 2.4 GHz band [11]. The CST simulated antenna is working well on the Bluetooth frequency range, and its resonance frequency is similar to the result obtained from the physical antenna measurement.

Figure 15 shows the CST modeled antenna result and physical measurement antenna result for the white wired inverted antenna which is connected to the 5 GHz Wi-Fi radio in the wireless router. Its deepest resonance during the antenna measurement was at 5.492 GHz. During the physical antenna measurement, many “humps” were seen above the 5 GHz Wi-Fi band where the return loss is larger than -10 dB, which was also seen in the CST Modeled Antenna. But overall the antenna works well in the designated 5GHz band. The resonant frequency of the CST modeled antenna was seen to be around 4.8 GHz, which is less than that obtained from the physical antenna measurement. The same kind of measurement error seen in the case of the green wired bowtie antenna might be the cause for the deviation in the resonant frequency between the two sets of data. However, we hope to modify the antenna in such a way that we would be able to select the desired resonant frequency for the modified antenna.

After the return loss measurement, we further investigated the far-field radiation patterns for both the physical antennas as well as the CST modeled antenna. The radiation pattern plot allows us to visualize the direction where the antenna transmits or receives power. This power variation as a function of the arrival angle is observed in the antenna's far field [9]. The radiation plot data was taken inside the anechoic chamber and the data was exported from the network analyzer to a digital file. Similarly, the radiation pattern data of the CST modeled antennas were

also exported from CST Microwave Studio. These two sets of data were imported to Python Programming language and plotted in the same plot so that they can be compared to see the similarity and discrepancy in the radiation pattern of the two antennas. This process was repeated for each of the antennas. Since the green and the blue antenna are dual-band Wi-Fi antennas, the radiation pattern data for those antennas were taken in each frequency. The radiation pattern plots for the antennas are shown in figure 16-22. The physical antenna measurement result is shown in dashed blue color while the CST modeled antenna result is shown in the solid orange colored curve.

RADIATION PATTERN PLOTS: MEASURED VS CST SIMULATED ANTENNAS

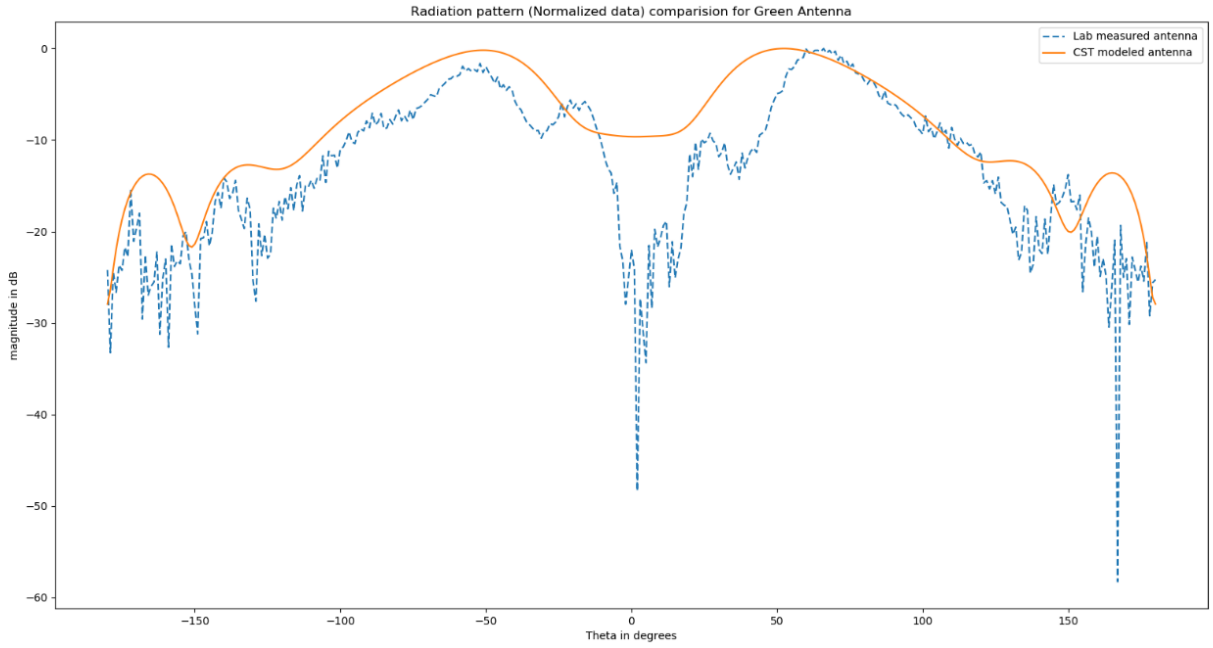

Figure 16. Radiation Pattern Plot for Green Wired Antenna at 5.4 GHz Frequency

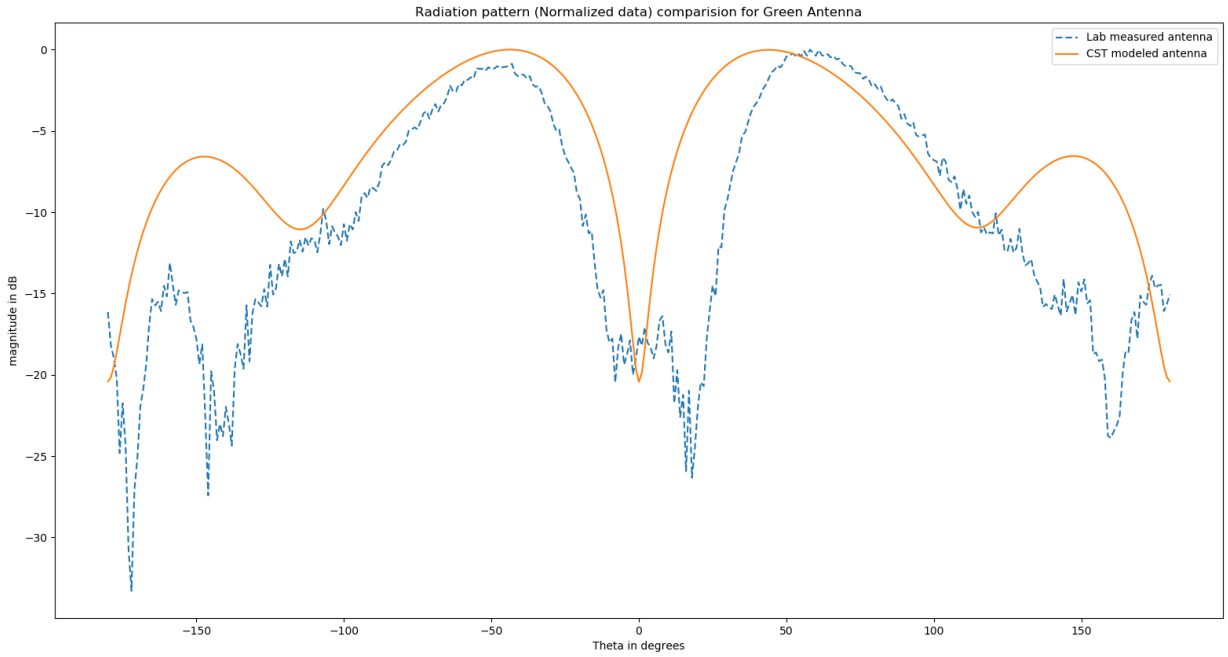

Figure 17. Radiation Pattern Plot for Green Wired Antenna at 2.4 GHz Frequency

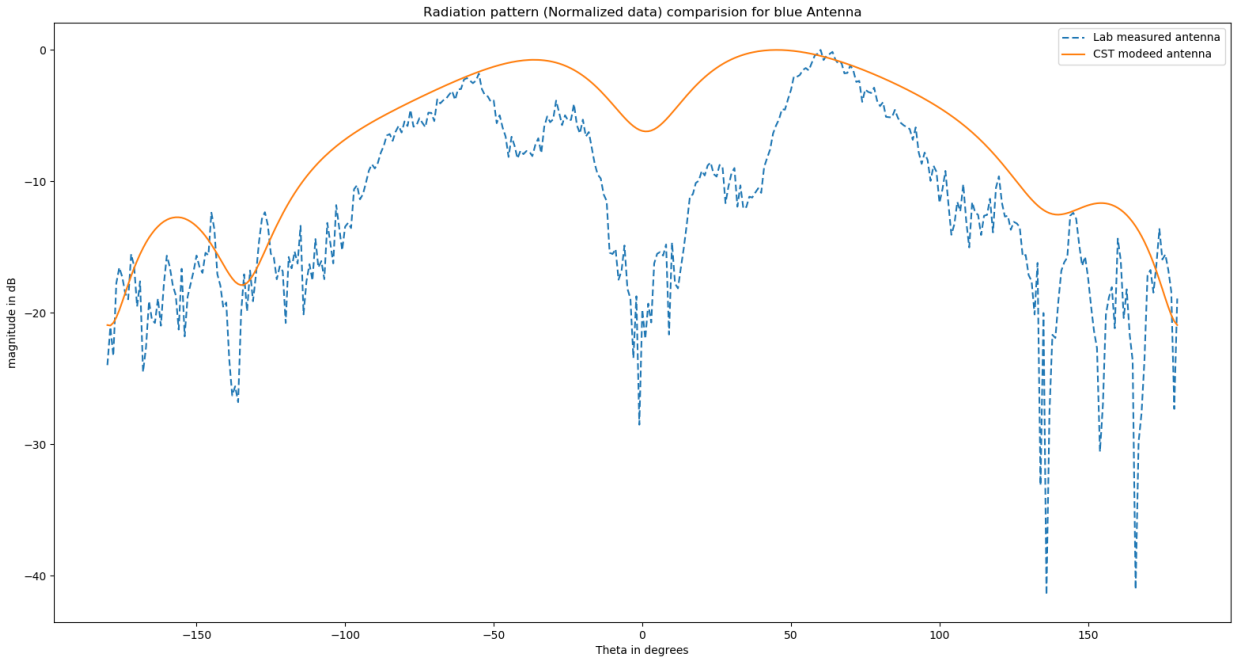

Figure 18. Radiation Pattern Plot for Blue Wired Antenna at 5.7 GHz Frequency

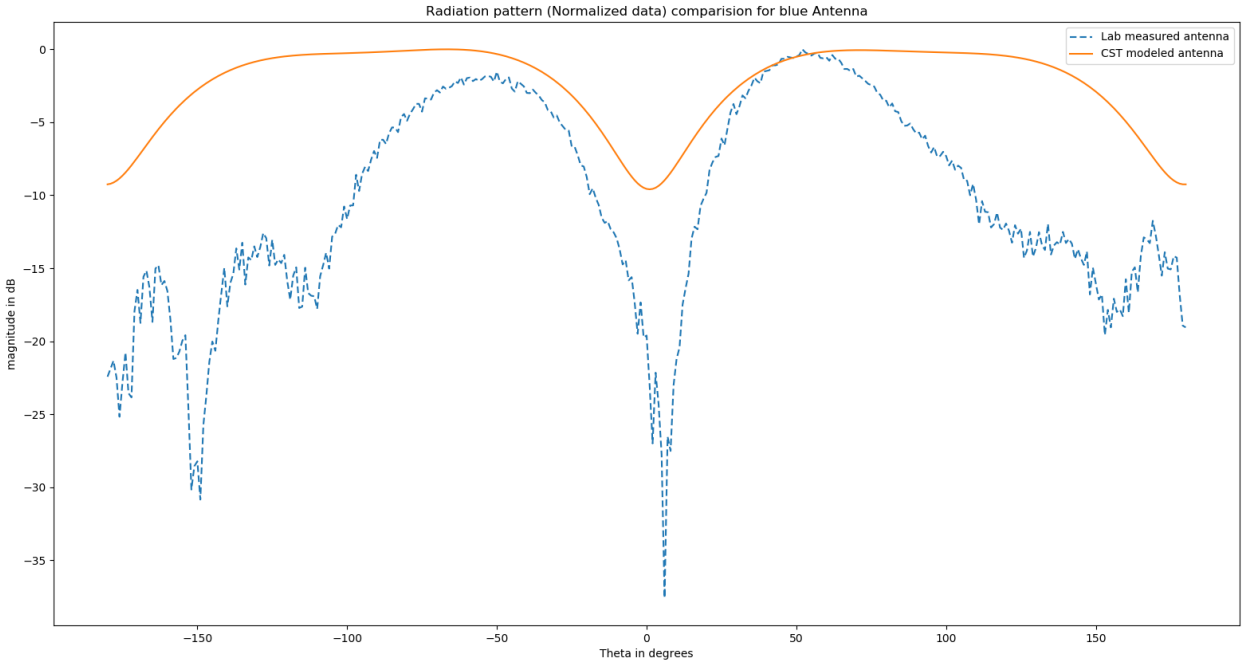

Figure 19. Radiation Pattern Plot for Blue Wired Antenna at 2.6 GHz Frequency

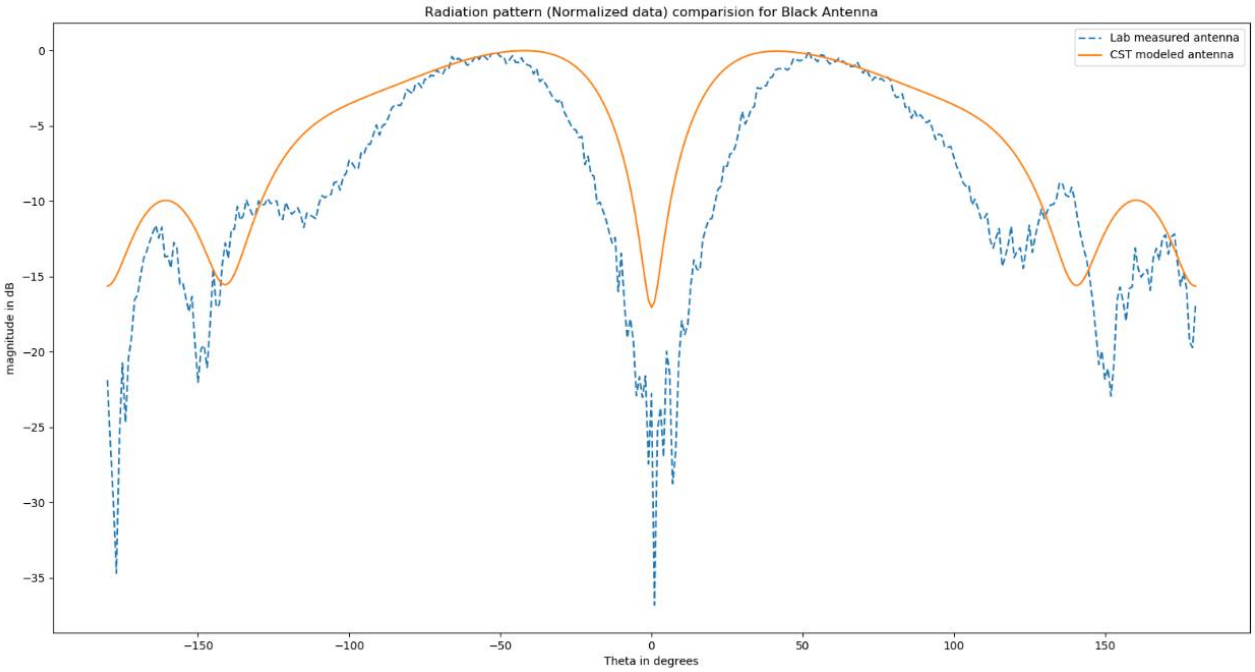

Figure 20. Radiation Pattern Plot for Black Wired Antenna at 2.5 GHz Frequency

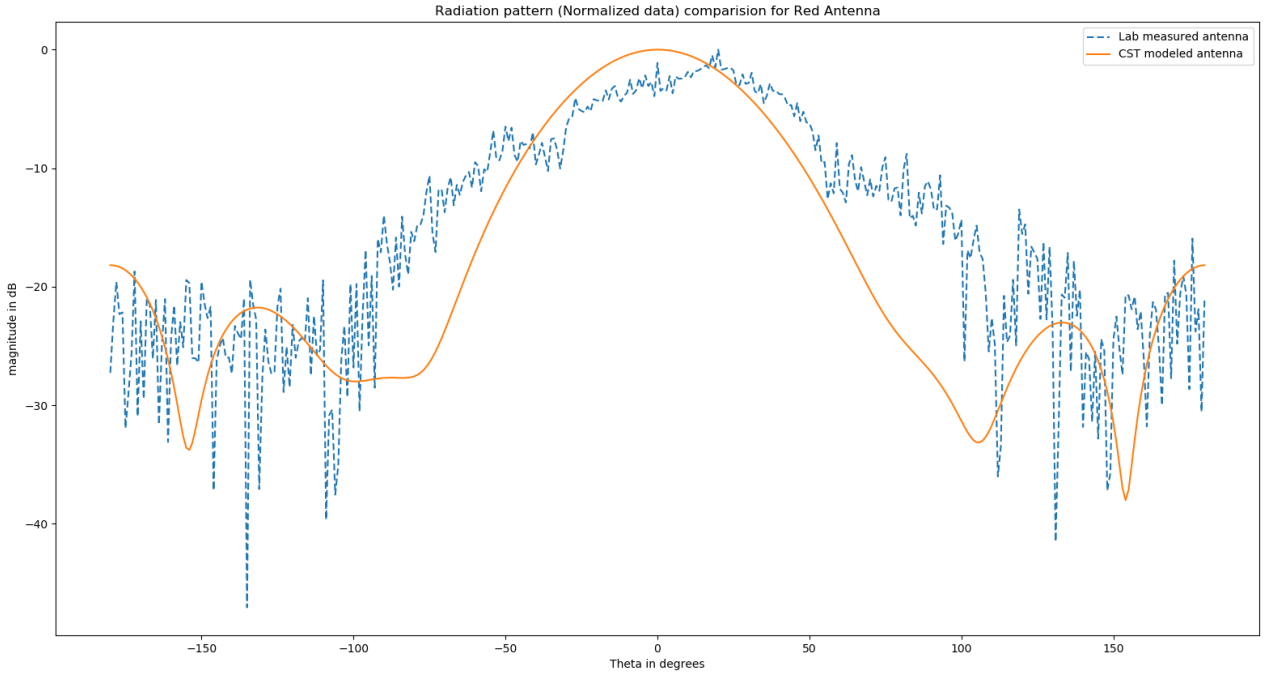

Figure 21. Radiation Pattern Plot for Red Wired Antenna at 2.7 GHz Frequency

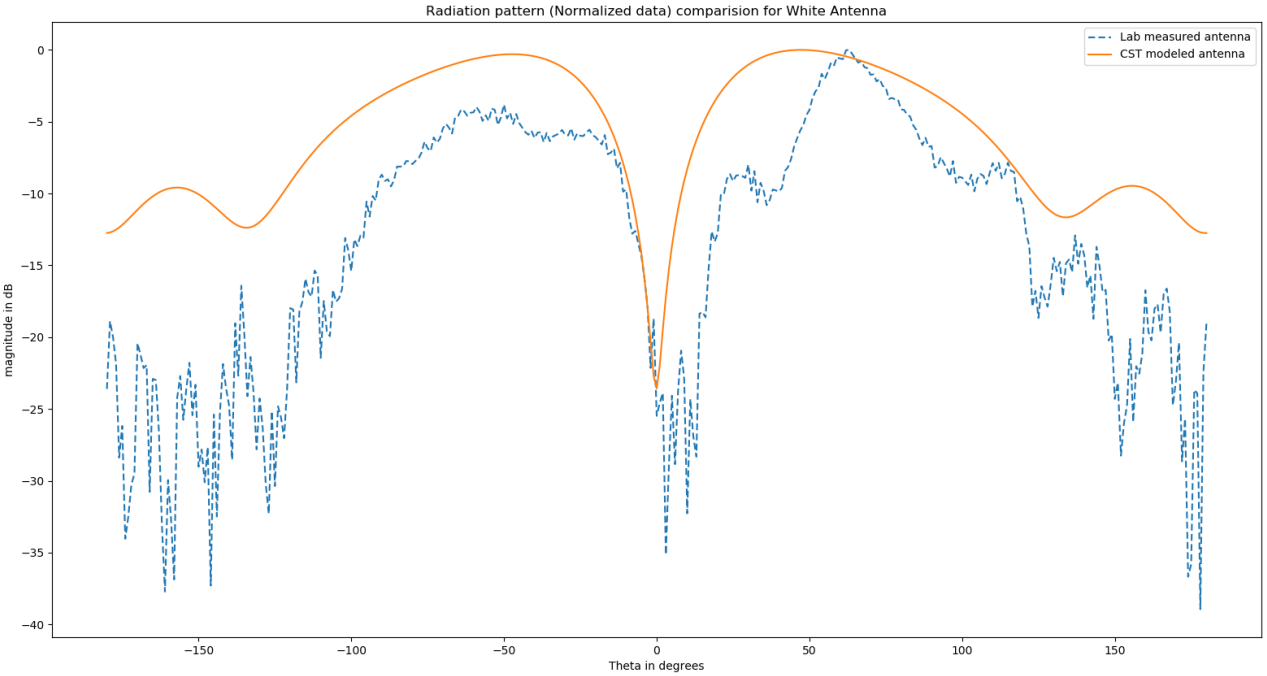

Figure 22. Radiation Pattern Plot for White Wired Antenna at 5.5 GHz Frequency

Figure 16-22, shows the normalized radiation pattern plots for the five different antennas. The radiation pattern data obtained from the physical measurements and the data obtained from the simulation of the CST modeled antennas are in decent agreement with each other. The direction in which the power was intended to be radiated matched in both of the cases showing that the CST modeled antennas are a good replica of the physical antennas. We will now take these CST modeled antennas and modify them to manufacture them with the process of additive manufacturing.

The crucial steps start from here where we have to modify the antennas in such a way that the performance remains more or less similar to the original antennas, but the antenna manufacturing has to be attainable through the 3D printing method. And before we dive into the 3D printing antenna performance, it would be effective to see the steps and modification that needs to be implemented for 3D printing.

MODIFICATION FOR 3D PRINTING

As we have discussed, 3D printing works with step-by-step deposition of the material in layers to build a solid structure. This means that if we consider the bottom layer to be first layer and the layer above it as the second, the first layer should already be printed first to provide mechanical support for the molten metal ink to reside on top of the first layer. This will be then the second layer on top of which the next layer is built. If there is no mechanical structure beneath a layer to be printed (built) then that layer cannot be printed at all. That is why our original antennas of the wireless router need support to build the parts of the structure that do not have support beneath them. Let us consider the red antenna as shown in figure 23. The top layer consists of two

metal arm structure that does not have support below them. Such structure cannot be manufactured by the additive manufacturing method without adding structural support.

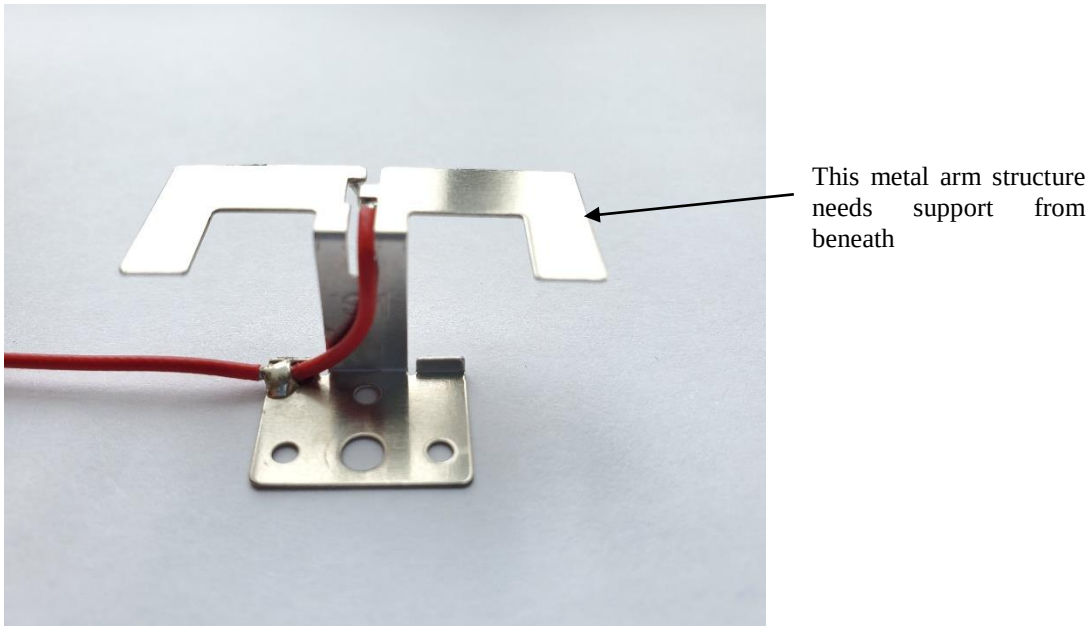

Figure 23. Explaining the Need for Support Structure during the 3D Printing Process

There are two ways to support such structures that do not have metal layers below them. The first way is to place a frame at an appropriate height over which the metal layer (that doesn't have support from beneath) can be printed by the printer's nozzle. The difficulty in using this method is that the support frame has to be placed at an appropriate height which might be sometimes very difficult to adjust for a miniature antenna structure. As the printed metal layer sticks to the frame, it might also not be possible to remove the frame and this new frame structure can also cause variation in the antenna characteristics. So, it is necessary to be careful that such

support frame structure doesn't bring about a change in the desired antenna characteristics since such structures are not generally considered during the antenna design.

The second method is to design the antenna structure along with a dielectric substrate that serves as the support structure for the antenna. The dielectric substance fills the air gap that is present in the antenna as shown in figure 24. As seen in figure 24, this time there is the dielectric substrate beneath the top layer that consists of two metal arm structure. This dielectric substrate acts as a layer on top of which the topmost metal layer can be printed.

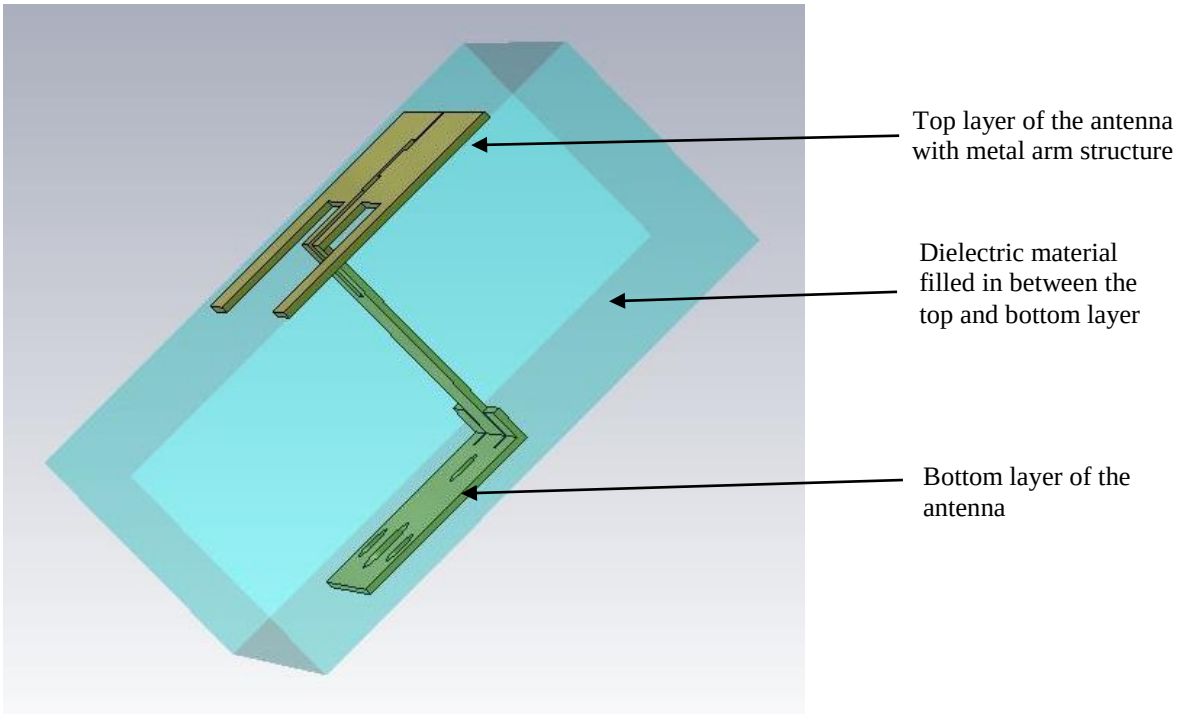

Figure 24. 3D View of the Red Wired Antenna Along with the Substrate (in Blue Color)

3D printing software slices the vertical height of the antenna into numbers of horizontal layers that are printed each at a time on top of one another. So, by this design procedure, we can make sure that there is always a flat horizontal layer along the width of the antenna whenever we are printing a top layer. This design procedure also precludes the need for the external support structure and the whole antenna structure can be manufactured easily with the 3D printer. Modern 3D printers are capable of printing two of these materials, namely, build material and the support material, simultaneously. The build material is the actual metal structure of the antenna while the support material is the dielectric substance that covers the air gap in the antenna and provides a layer for the build material to reside on top of. One thing to note is that the support material also provides mechanical support to the delicate antenna structure from bending and other damages.

Due to the convenience in manufacturing, we have used the dielectric support method in all our 3D printed antenna designs. While it is convenient to use such a method, the addition of the dielectric material in the antenna causes an expected change in the resonating frequency and the magnitude of the return loss of the antenna. This happens because the dielectric material reduces the speed of an electromagnetic wave radiated by the antennas. For our 3D printed antenna design, we have taken a dielectric material with relative permittivity of 2.45.

The speed of an electromagnetic wave in the dielectric material is given by:

$c = \frac{1}{\sqrt{\epsilon\mu}}$ where, ϵ is the permittivity of the dielectric substance and

μ is the permeability of the dielectric material

In our case, the permeability of the material is assumed to be same as that of the free space but the permittivity of the material is 2.45 times the permittivity of free space, hence the speed of the wave, therefore, decreases by a factor of $\frac{1}{\sqrt{2.45}}$

As the speed of an electromagnetic wave decreases, the decrease in frequency and wavelength compensate for this decreased speed. This is why the resonant frequency decreases after the introduction of the dielectric substrate. The dielectric material also causes a variation in the magnitude of the return loss, sometimes the magnitude was seen to decrease while at other times it was seen to increase as well.

To demonstrate the effect due to the addition of the dielectric material, we have taken the red antenna with the dielectric substrate placed as shown in figure 24. We then varied the relative permittivity of the dielectric material that was placed between the top and the bottom layer of the red antenna. By varying the relative permittivity of the dielectric material we can simulate different dielectric substrates. Simulations were then carried out for different values of the relative permittivity for the dielectric material. The different values of relative permittivity cause the best

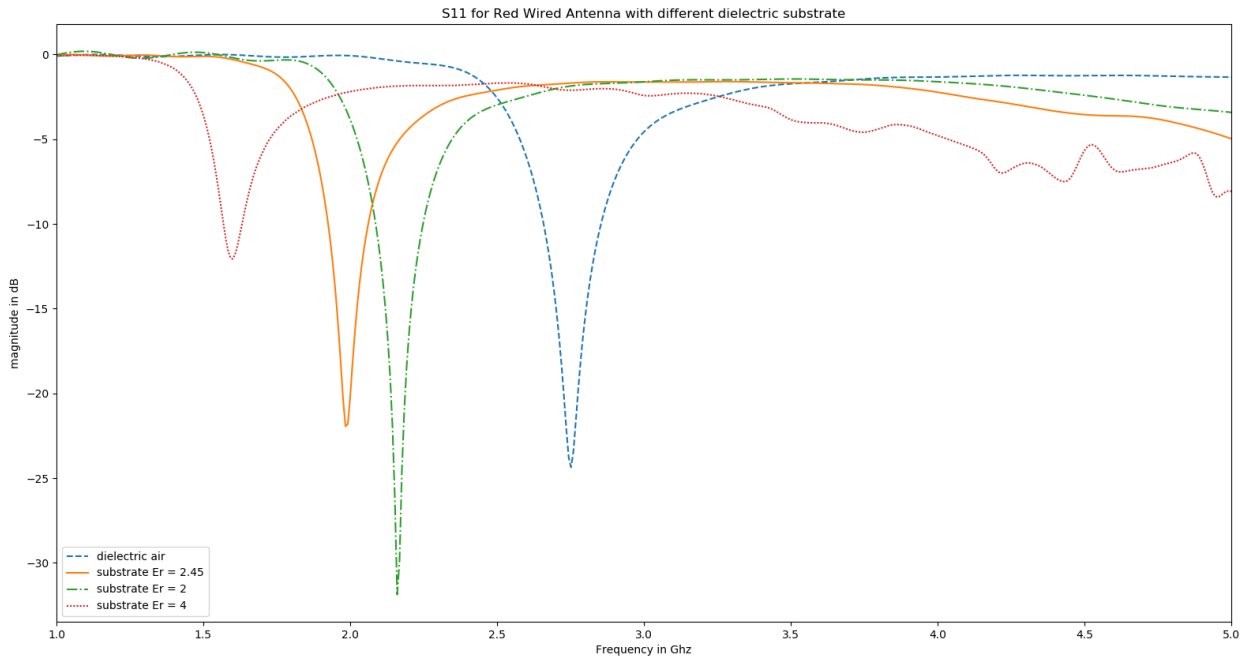

Figure 25. Comparison of S_{11} for Air vs. Different Dielectric Substrate Material

operating frequency of the antenna to differ accordingly.

As seen above from figure 25, which compares the S_{11} for different dielectric substrates versus the case of having air as the dielectric material. The dashed blue curve represents the case of having air as the dielectric substrate which also represents the original CST modeled red antenna whose performance is similar to the physical red wired antenna. The green, orange, and red curves are the S11 measurements when the dielectric material of relative permittivity 2, 2.45, and 4 are taken respectively. We can clearly see that the introduction of the dielectric substrate decreases the resonating frequency of the antenna. From figure 25, we can see that as the permittivity of the material increases, the resonant frequency (or the best operating frequency) of the antenna also decreases. The resonant frequency for the antenna with air as the dielectric material is seen to be around 2.75 GHz. This resonant frequency lowered to 2.15 when we used material with relative permittivity of 2. For the relative permittivity of the material set to 2.45 and 4, the resonant frequency was seen to be 1.98 and 1.59 respectively. As mentioned earlier, in our case for the 3D printing process, we have taken a dielectric material with relative permittivity of 2.45. So, after the introduction of the dielectric material with relative permittivity 2.45, the resonant frequency of the antenna lowered to 1.98 GHz. Also, it is seen that the dielectric substrate brings an erratic variation in the magnitude of the return loss at the best operating frequency. In summary, we can say that the antenna is unfit to use in the intended frequency after the introduction of the dielectric material. This was the exact problem we were facing in designing the antenna to be suited for 3D printing.

To tackle this problem, we came up with two solutions. The first one was to scale the size of the antennas. We know that the physical size of the antenna is directly related to the wavelength of the antenna. Generally, the higher is the resonant frequency the antenna size diminishes and

vice versa. In our case, due to the introduction of the dielectric substrate, the resonant frequency had lowered more than what was required, it was necessary for us to scale down the size of antennas modeled in CST Microwave Studio. To achieve this, we reconstructed the CST modeled antenna again one more time but included a scaling factor into the antenna dimension at that time. By this, we mean that, if the original dimension measured by the Vernier calipers was 20 mm then the CST model was constructed with a parameter b*20 mm where "b" is the scaling factor for the design. The value of b can be anything other than 0, and with each "b", we can make an antenna with identical design and structure but with different dimensions. The ingenious solution to obtain the correct value of "b" was by intelligent guess as well as with the help of the parameter sweeping feature of the CST, which allows the value of the parameter to be modified and run a simulation to calculate the antenna performance for each of the values.

The scaling factor was mostly accurate to tune in the antennas to the selected resonant frequency. We could easily shift the resonant frequency by changing the scaling factor. Along with a proper resonant frequency, we also required a good return loss (less than -10 dB) to be observed at the resonant frequency. Attainment of these conditions was particularly difficult with the white wired antenna and the dual-band green wired antennas.

The wireless router antennas were designed for a particular frequency and condition, which is why adding dielectric material and scaling them leads us to the correct resonant frequency but it is difficult to obtain good performance characteristics in that particular resonant frequency. That is why it was necessary for us to understand the working of the antennas and which particular structure in the antenna defined the resonance frequency, gain, and other performance matrices of the antenna. Mastering this helped us to design a general green wired antenna that may not exactly look like the original antenna but retained most of the overall structures and showed good

performance characteristics over the desired frequency of interest.

Another approach we took to address this issue of not having good performance in the best operating frequency was the ingenious placement of the dielectric material. By this, we mean that the dielectric material support was provided only to those metal components which do not have a support layer below them. Instead of filling the dielectric material whole over antenna structure between the top and the bottom layer as in figure 24, the dielectric material was used only in those places required to support the top metal structure. As shown in figure 26, we have not placed the dielectric material inside the rhombus because there is not any metal layer over it requiring support. Similarly, the plate with three circles in figure 26 also doesn't need any support during printing as it itself is the bottom layer of the antenna but the bowties structures were provided with dielectric substrate from the base of the antennas as shown in the figure.

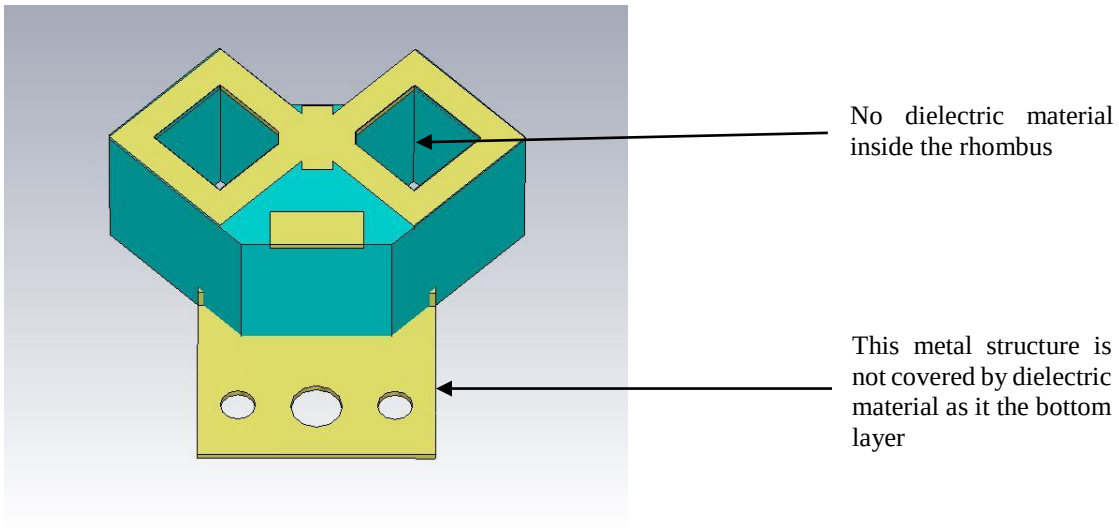

Figure 26. Ingenious Placement of the Dielectric Material

We used the above mentioned approach to design modified antennas which are shown in figure 27-31 on the following pages. The blue colored material is the dielectric material.

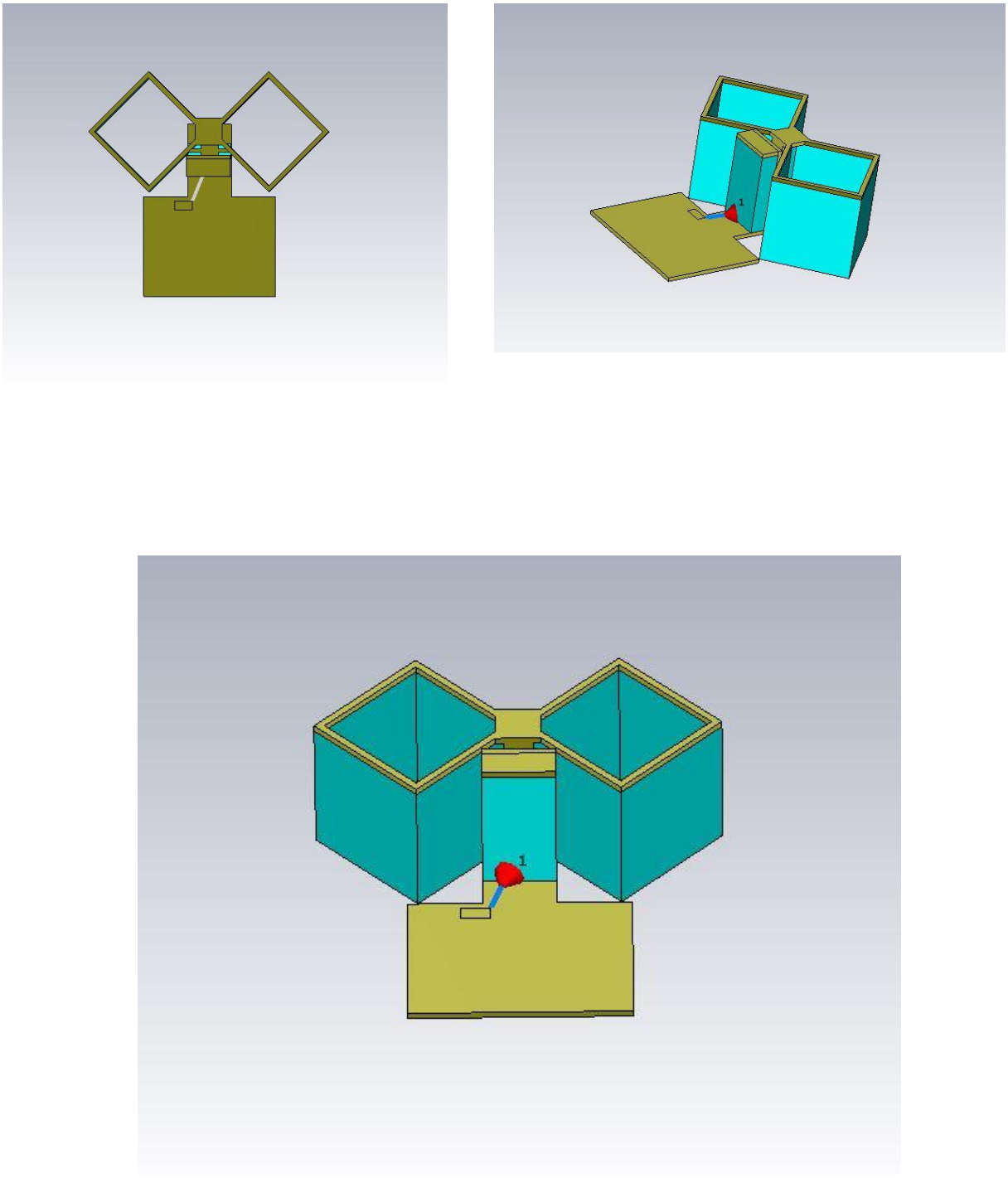

Figure 27. Green Wired Antenna with Dielectric Substrate Modified for 3D Printing

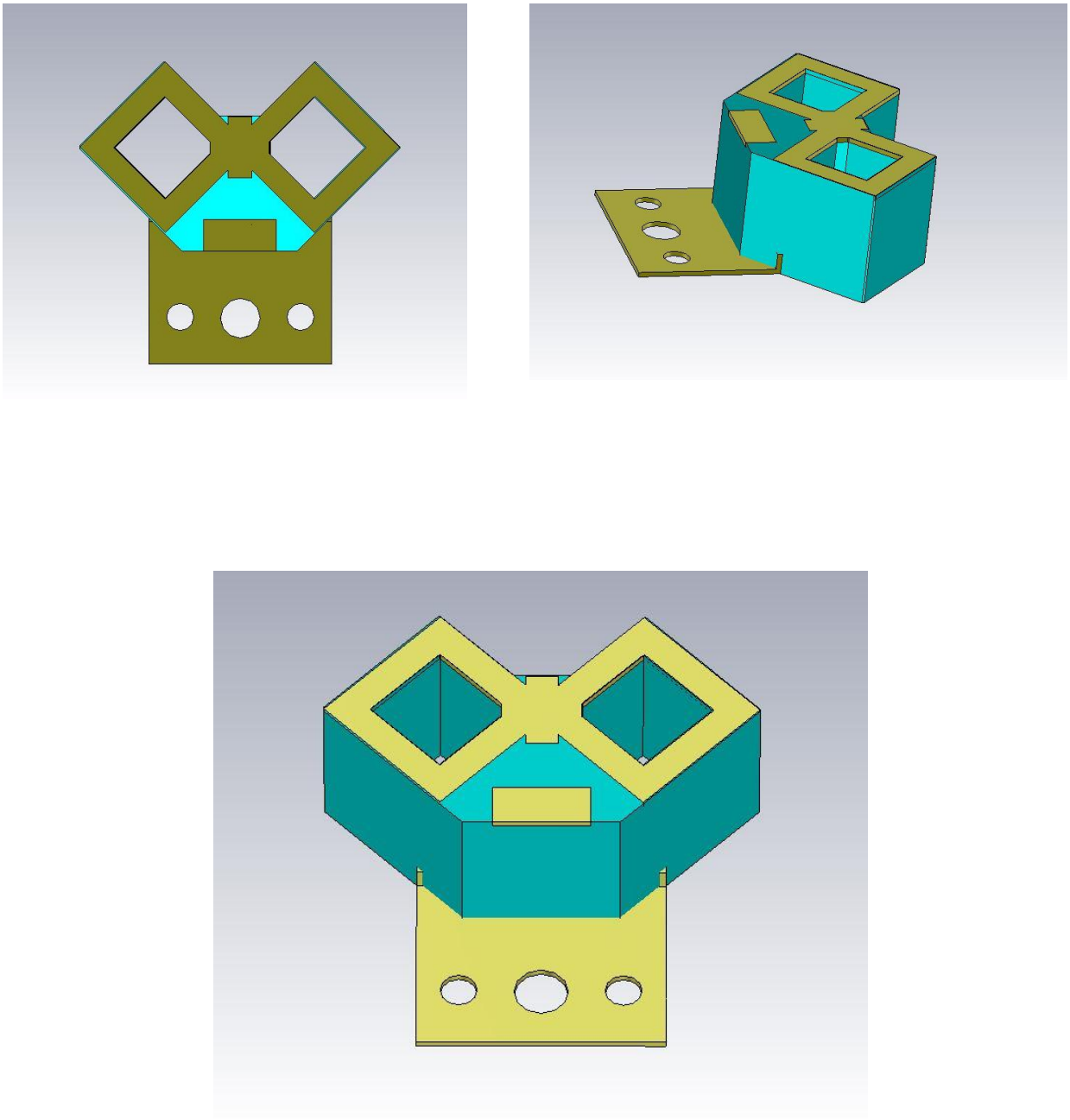

Figure 28. Blue Wired Antenna with Dielectric Substrate Modified for 3D Printing

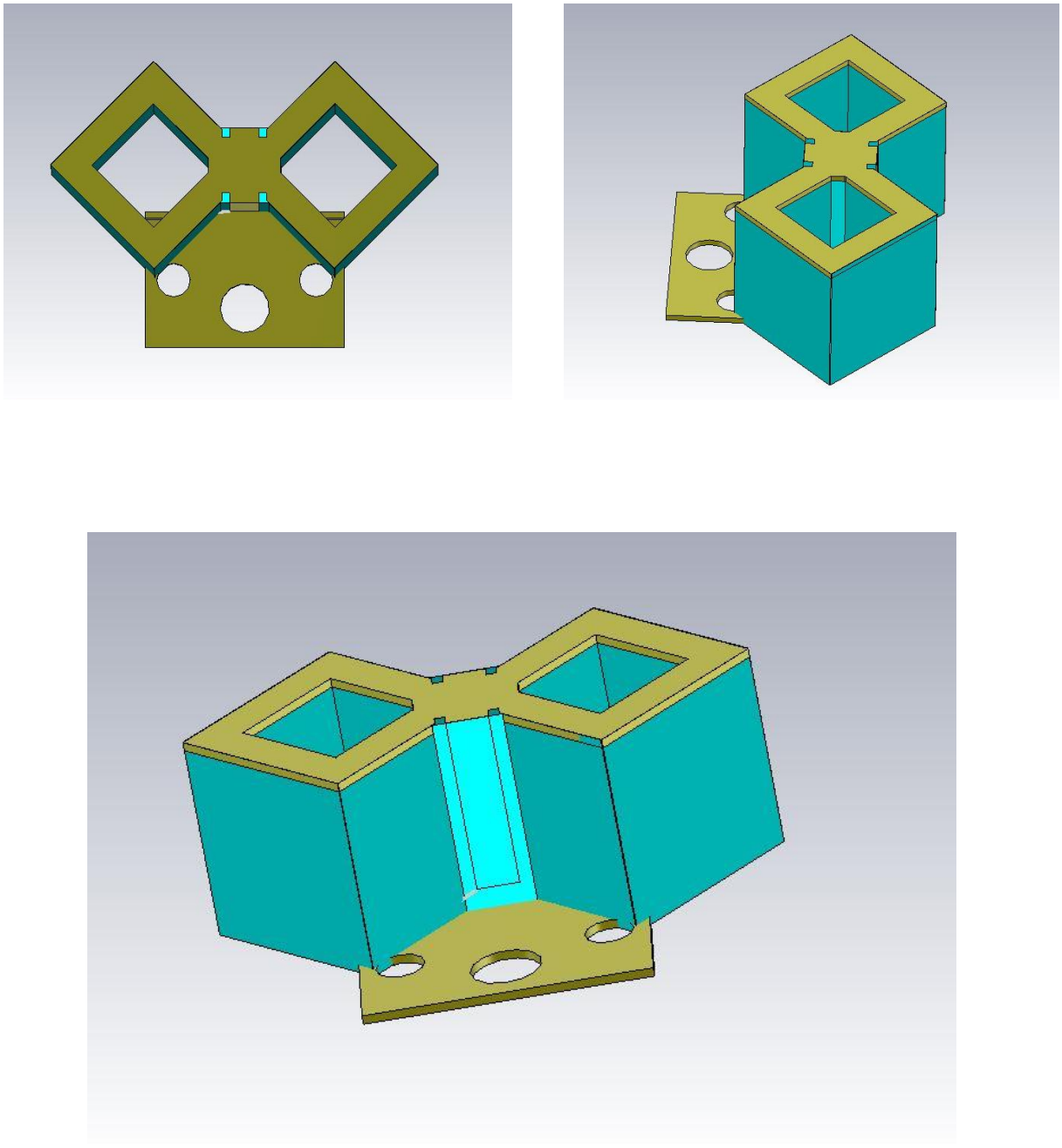

Figure 29. Black Wired Antenna with Dielectric Substrate Modified for 3D Printing

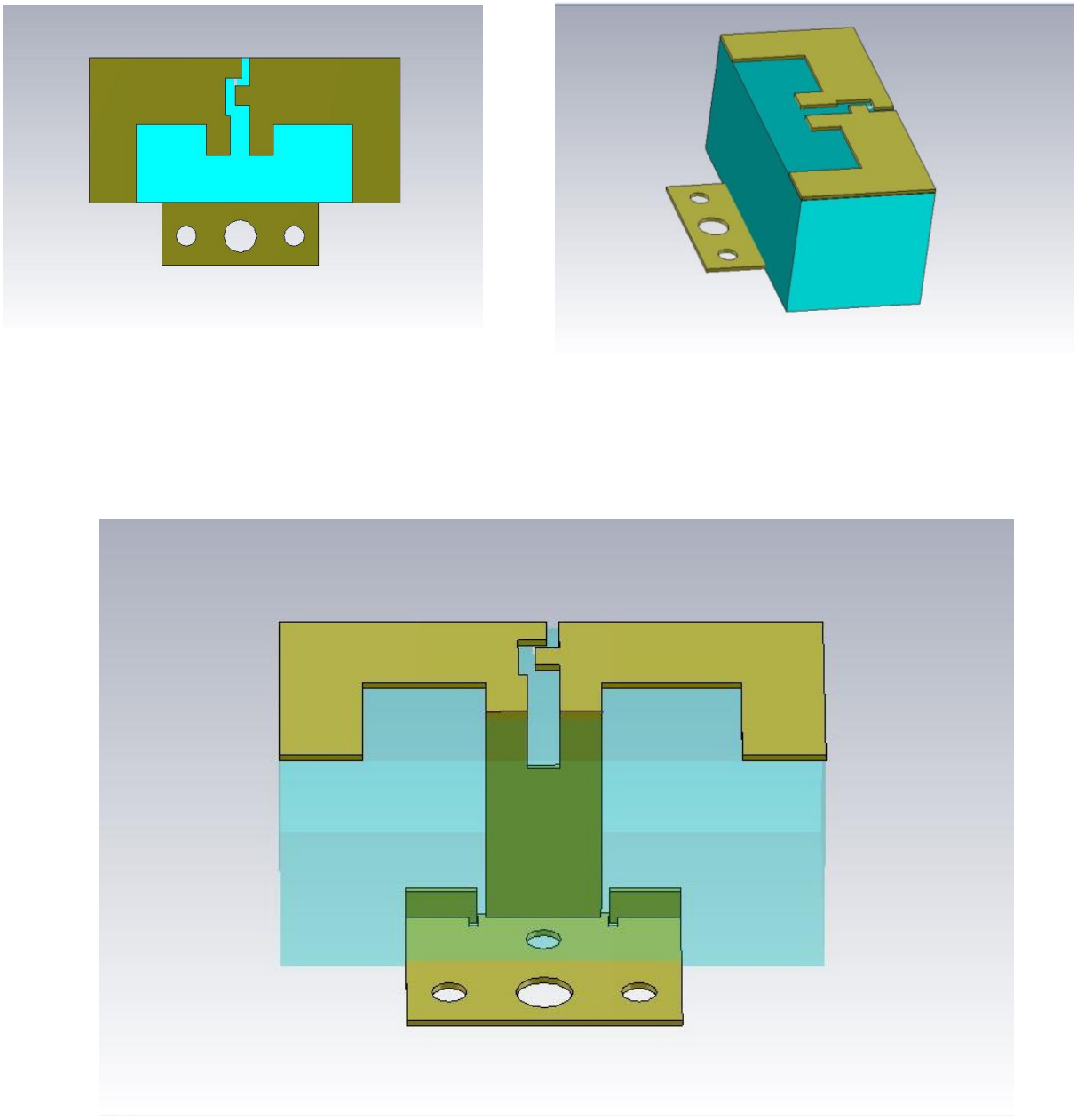

Figure 30. Red Wired Antenna with Dielectric Substrate Modified for 3D Printing

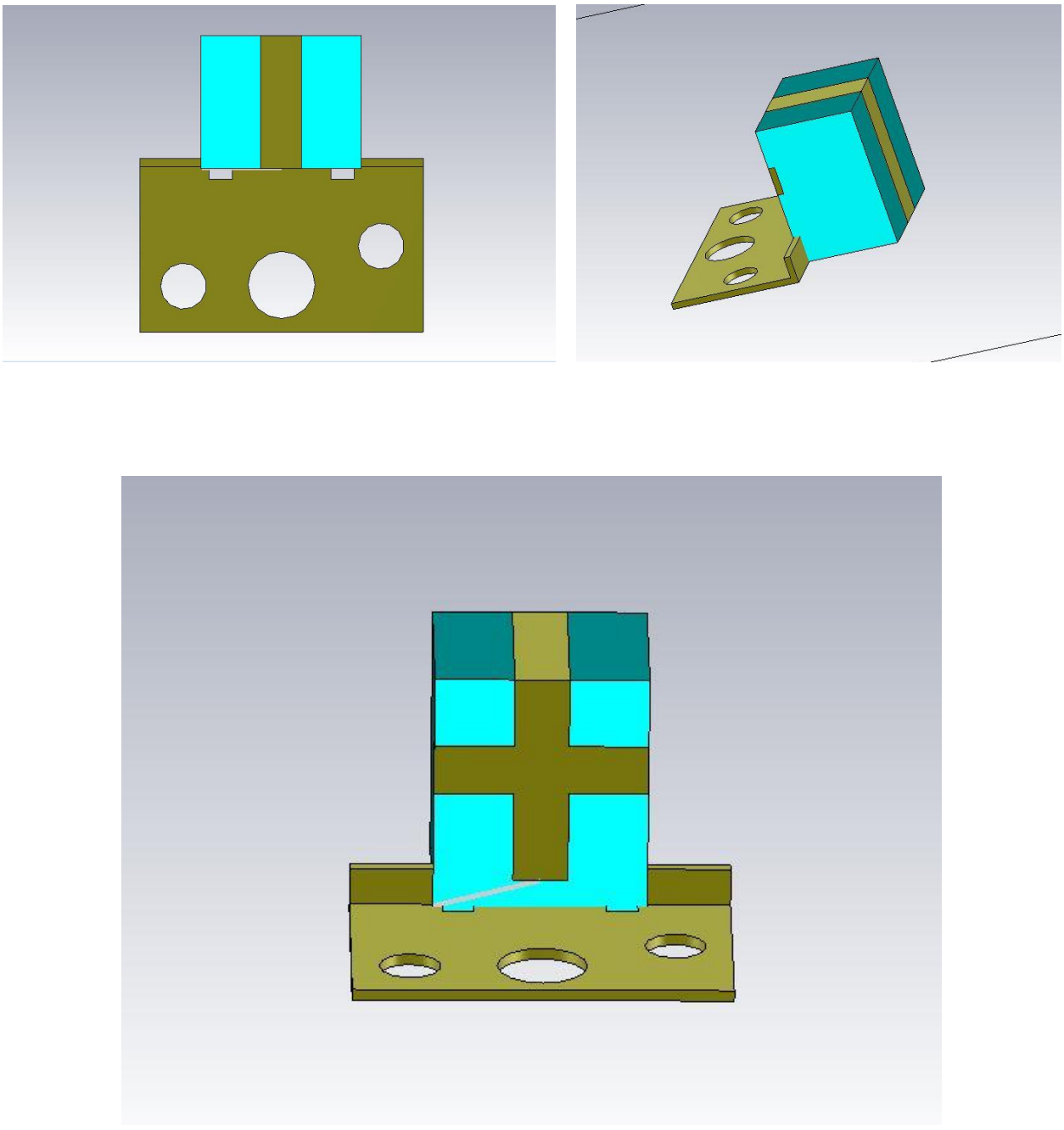

Figure 31. White Wired Antenna with Dielectric Substrate Modified for 3D Printing

CHAPTER IV

RESULTS OF MODIFIED ANTENNAS

As mentioned above in the working procedure, the technique of ingeniously placing the dielectric material between the top and the bottom layer of the antenna as well as the method of scaling the antennas to tune them into the desired frequency of interest were the most important ideas to design the 3D printed antenna. Although the magnitude of the return loss might be different in comparison to the results in case of the physical antennas, we still expect the antenna to have a good return loss (less than -10dB) at the resonating frequency. All of the five antennas were redesigned to be 3D printed in CST Microwave Studio and the antenna simulations were carried out setting up an environment to reflect the lab antenna measurements. We have used the return loss (S_{11}) and radiation pattern plots to compare the performance characteristics of the antennas. The return loss (S_{11}) obtained after modifying the antenna for 3D printing was compared with the CST modeled antenna to make sure that the newly designed antennas are on track with the desired performance level. We particularly selected the CST modeled antennas for comparisons because their results had smooth curves with little noise. The S_{11} for two data sets (modified antennas and originally CST modeled antenna) is plotted from figure 32 to figure 36 for green, blue, black, red, and white wired antenna respectively. The blue colored dashed curve represents the results for the originally CST modeled antennas while the solid orange curve represents the S_{11} results for the modified antennas.

S_{11} PLOTS OF ANTENNAS MODIFIED FOR 3D PRINTING

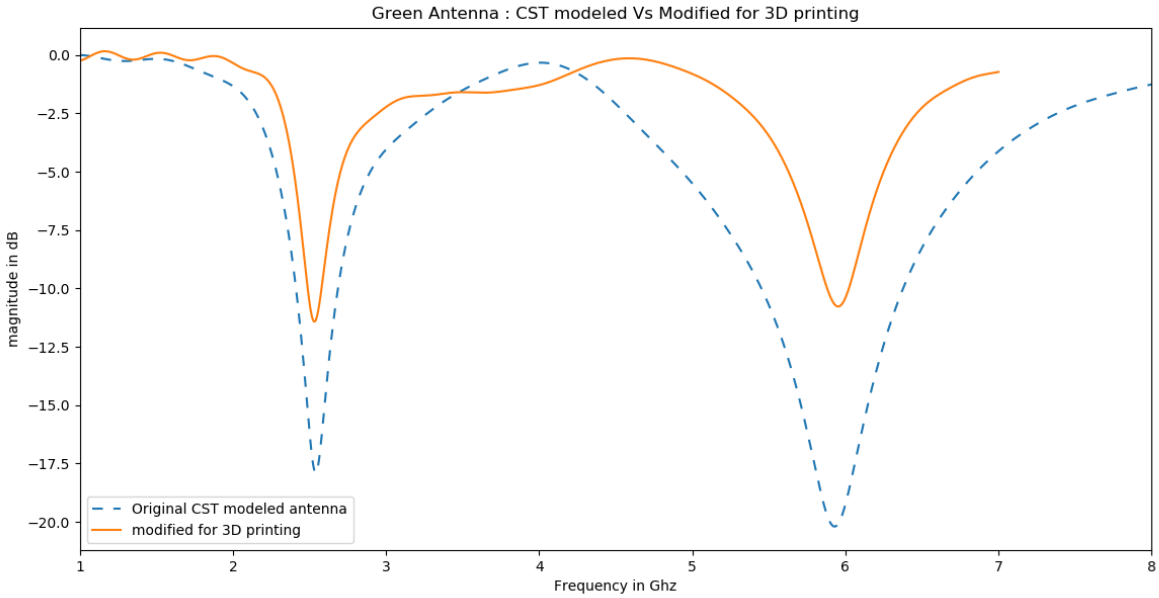

Figure 32. S_{11} for Green Wired Antenna, CST Modeled vs. Modified for 3D Printing

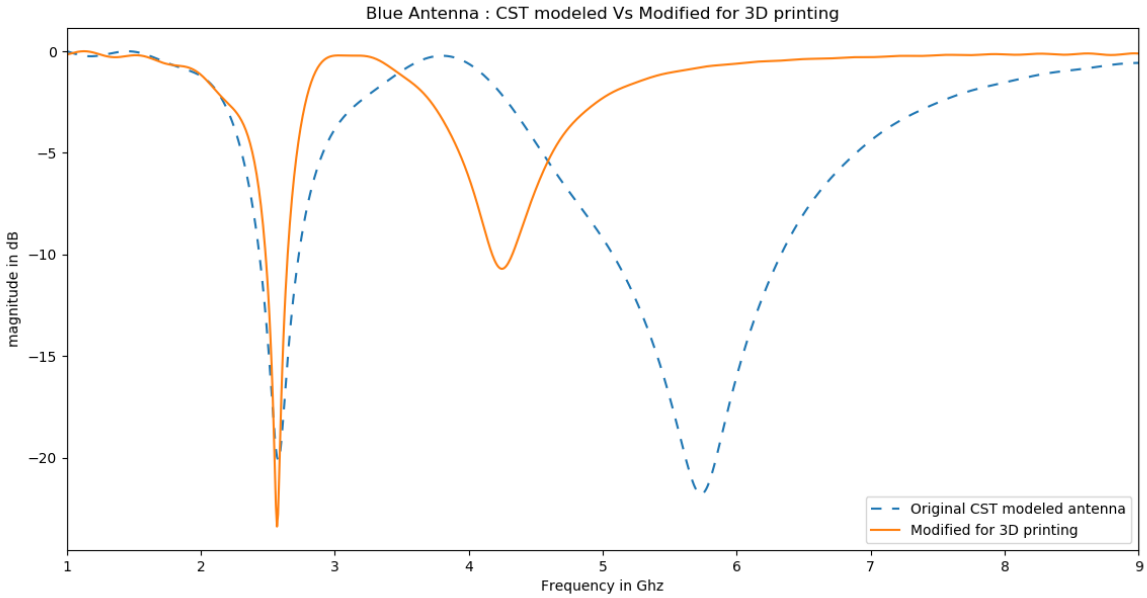

Figure 33. S_{11} for Blue Wired Antenna, CST Modeled vs. Modified for 3D Printing

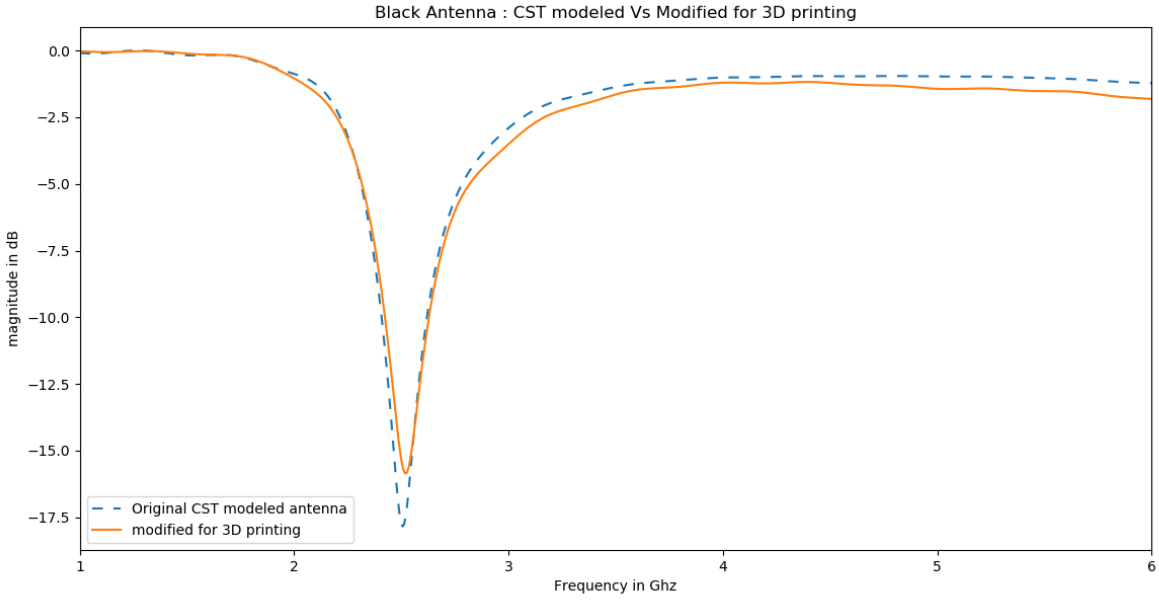

Figure 34. S_{11} for Black Wired Antenna, CST Modeled vs. Modified for 3D Printing

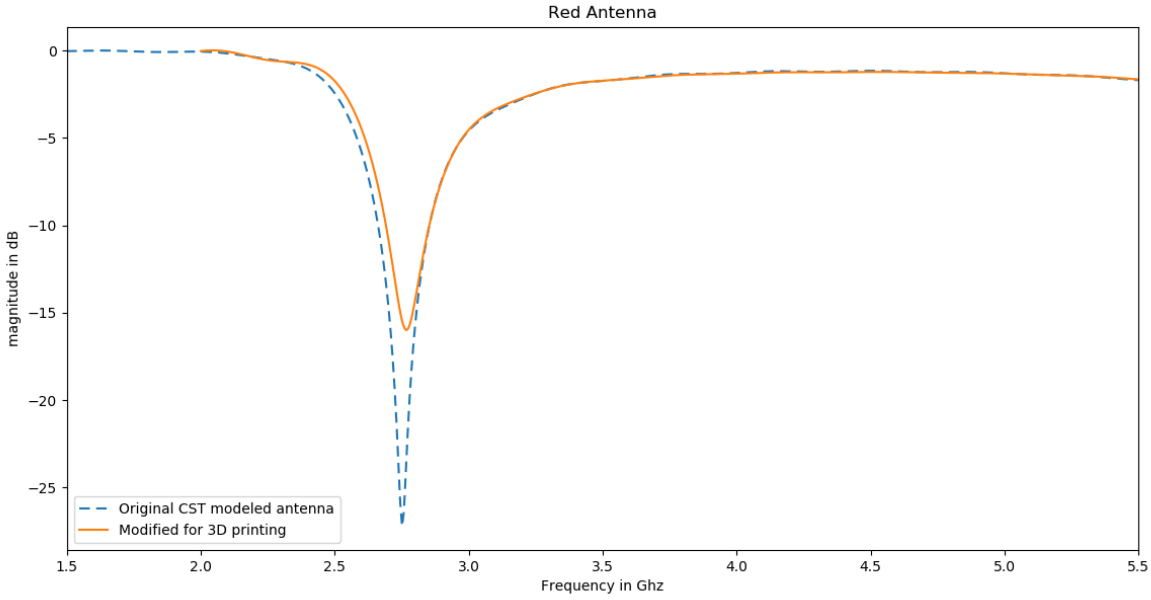

Figure 35. S_{11} for Red Wired Antenna, CST Modeled vs. Modified for 3D printing

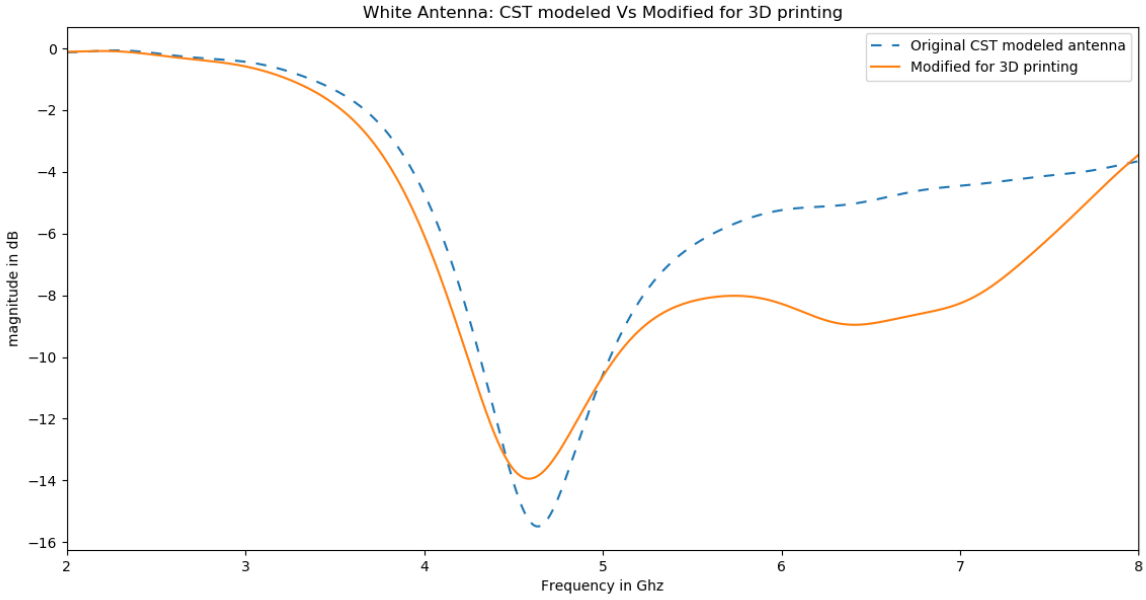

Figure 36. S_{11} for White Wired Antenna, CST Modeled vs. Modified for 3D Printing

After the S_{11} results, the results for the radiation pattern comparison is shown in figures 38-42. The radiation pattern result for the originally CST modeled antenna is shown by the blue dashed curve while the solid orange colored curve represents the result for the modified antennas for 3D printing. Chapter 5 discusses the results obtained from the S_{11} and radiation pattern comparison for the two antennas.

RADIATION PATTERN PLOTS FOR MODIFIED ANTENNAS

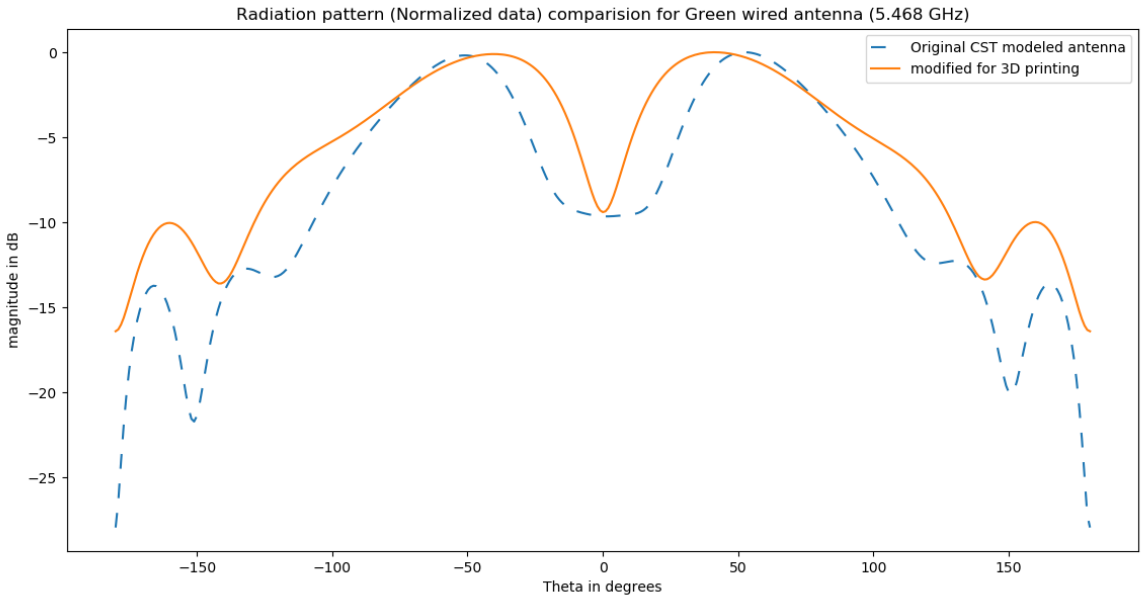

Figure 37. Radiation Pattern Plot of Modified Green Wired Antenna at 5.47 GHz Frequency

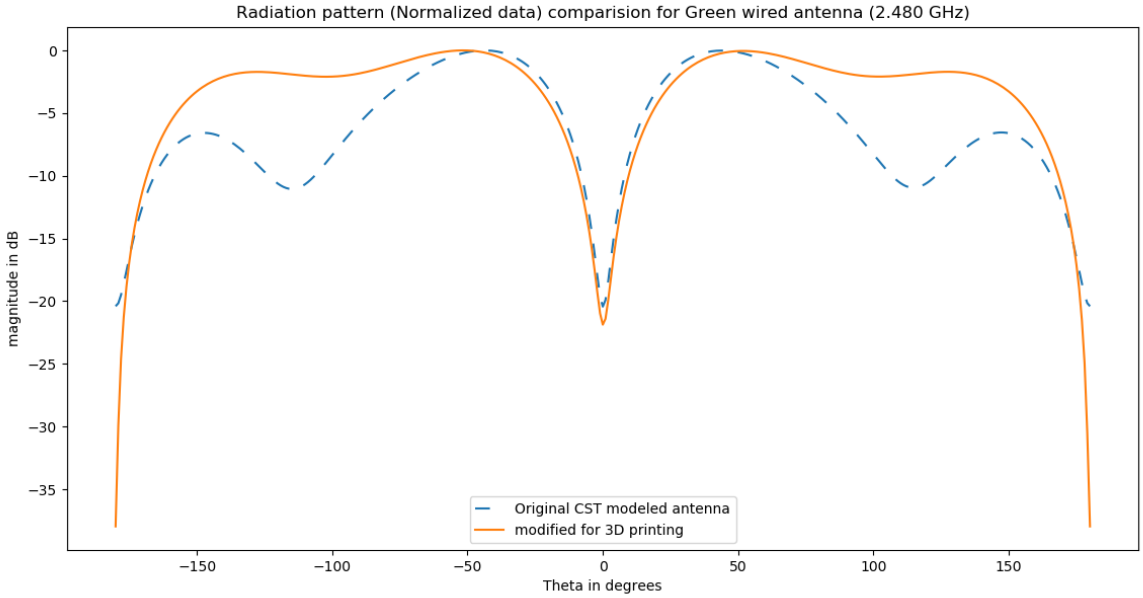

Figure 38. Radiation Pattern Plot of Modified Green Wired Antenna at 2.48 GHz Frequency

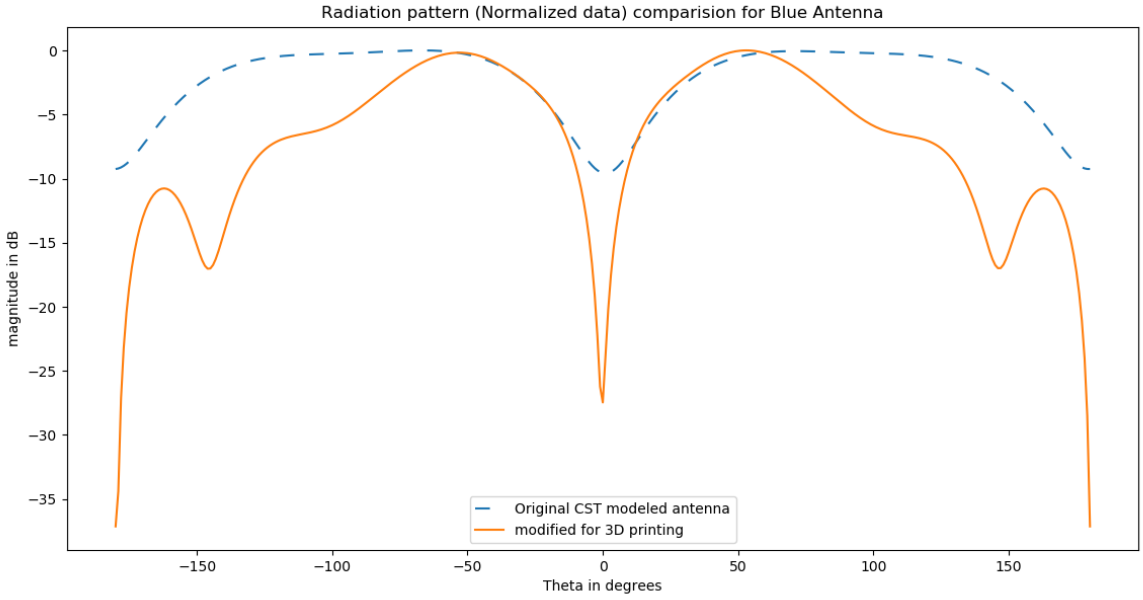

Figure 40. Radiation Pattern Plot of Modified Blue Wired Antenna at 2.6 GHz Frequency

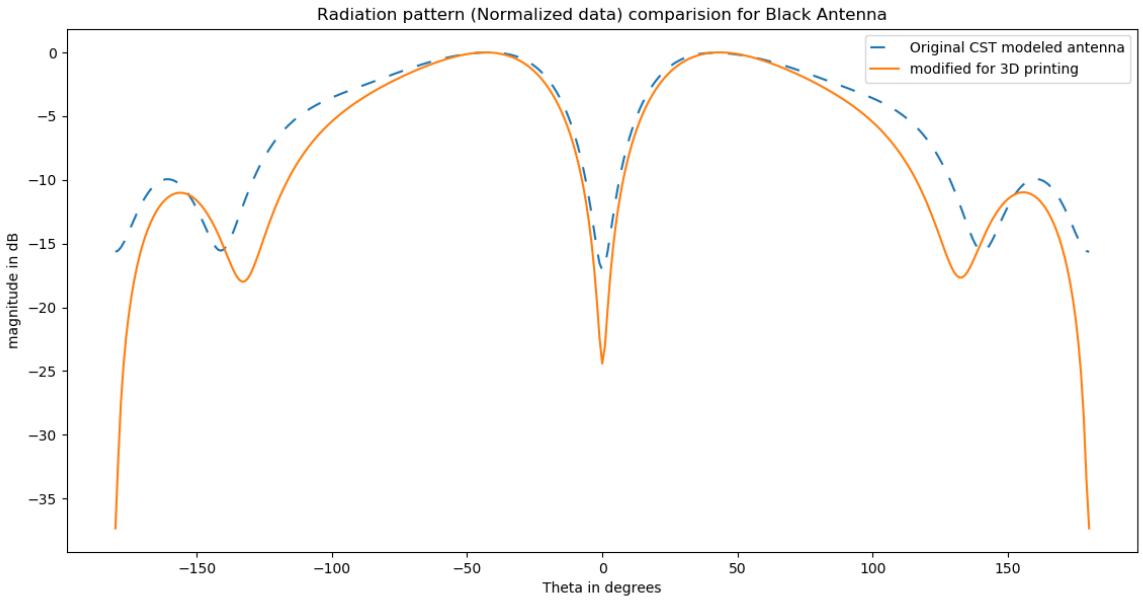

Figure 39. Radiation Pattern Plot of Modified Black Wired Antenna at 2.59 GHz Frequency

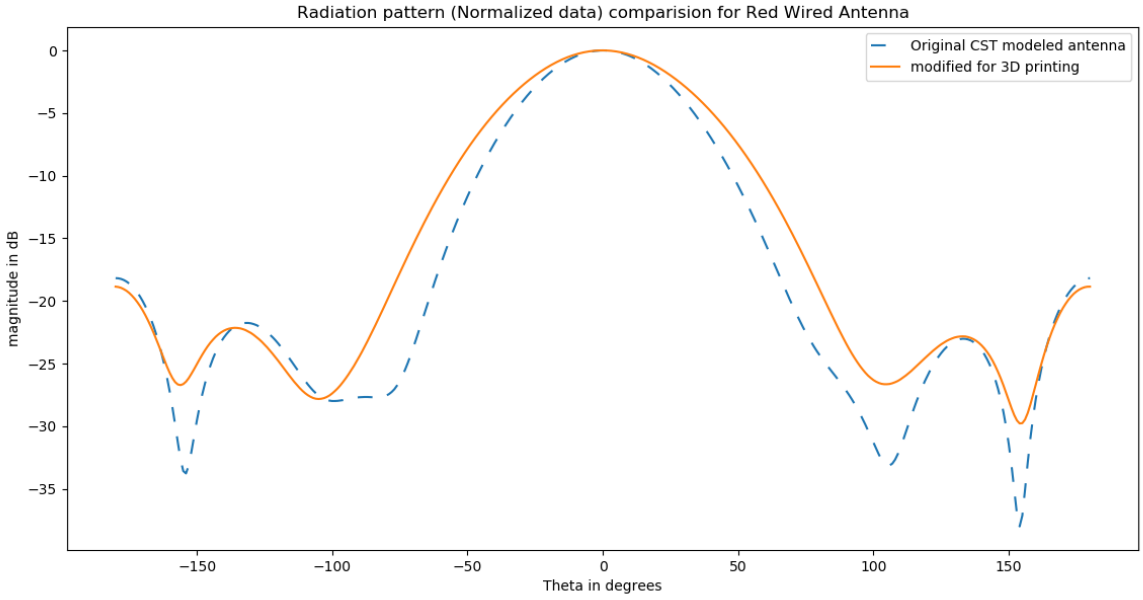

Figure 42. Radiation Pattern Plot of Modified Red Wired Antenna at 2.75 GHz Frequency

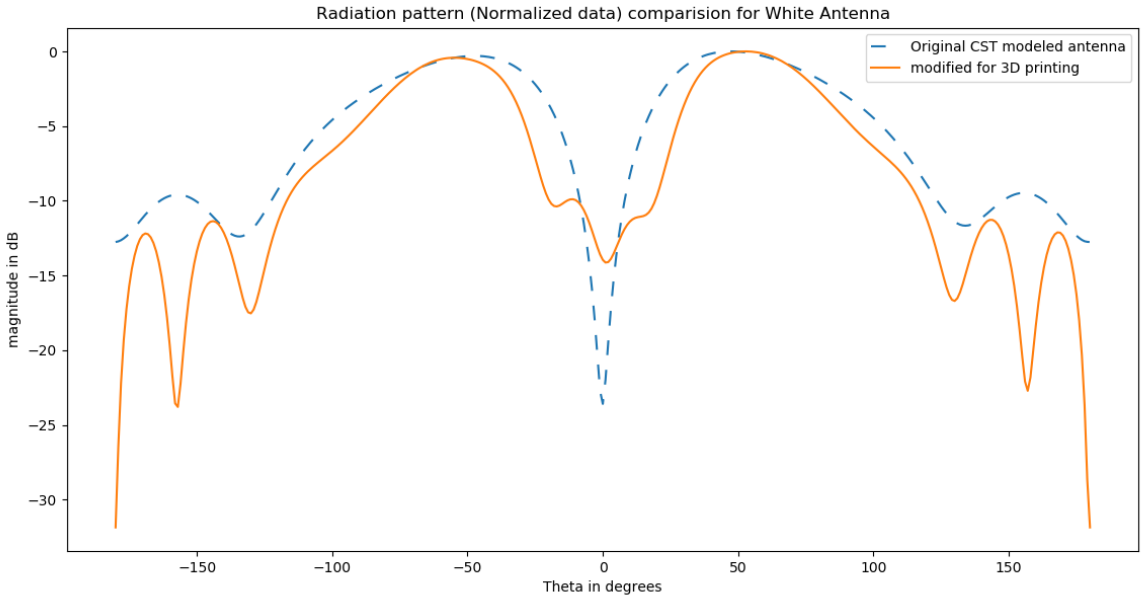

Figure 41. Radiation Pattern Plot of Modified White Wired Antenna at 5.49 GHz Frequency

CHAPTER V

DISCUSSION AND CONCLUSION

In this thesis, we modeled the antennas of a wireless router and made the adjustment in the design of the antennas so that the antenna can be manufactured with the method of additive manufacturing. The major difficulty in making a 3D printed antenna is that when an antenna is filled with a dielectric substrate, it decreases the resonant frequency of an antenna and deteriorates the magnitude of the return loss at the resonant frequency. In this case, a dielectric material with relative permittivity of 2.45 was used as a substrate to fill antennas and support the metal while printing. Thus, the use of appropriate dielectric substrate material is necessary in order to design a good antenna with good return loss at the resonant frequency.

The plots in the previous results section show antenna performance results. From figure 32-26, we can say that the modified antennas performance is in concert with the originally modeled CST antennas (which also represent the actual physical antennas). From figure 32, it can be seen that even though the resonant frequency in both the Wi-Fi band coincides, the green wired antenna has reduced magnitude of return loss in both the bands. Nevertheless, we are able to outperform the -10dB threshold that defines the return loss for a good antenna. The green wired antenna is a dedicated network sensor, so it is necessary that it has to resonate in the dual-band Wi-Fi frequency with good return loss. It was particularly difficult to modify the green antenna for 3D printing because it was necessary to operate in both Wi-Fi bands. Even a slight modification would change

one of the two resonating frequency and make the antenna unusable in both bands. So, the green antenna was again designed in such a way that every parameter could be modified in CST and new simulations could be run again to record the change. The green wired antenna that works in our case somehow retains the design of the original physical antenna but also differs in a lot of aspects. Likewise, the blue antenna is also a dual-band antenna but, in the router, it is only used for the 2.4 GHz Wi-Fi band. That is why we have optimized our 3D printed antenna to work well in that band only because we would lose the extraordinary performance it is showing currently in that 2.4 GHz band if we try to operate it as a dual-band antenna. The black wired antenna and the red wired antenna needed very little modification to optimize them for 3D printing. Scaling the antennas with the correct scaling factor easily accounted for the desired frequency range with good return loss measurements, which can be clearly seen in the plots above for the red wired antenna and the black wired antenna. Finally, it was rather difficult to design the white antenna with good return loss in the 5 GHz Wi-Fi band, as scaling the original model was not yielding a return loss less than -10 dB. After several design modifications, the adjustment in the width of the front horizontal structure finally gave a result needed to establish it as a good antenna in the 5 GHz range.

To make sure that an antenna is a good radiator it is essential that the return loss of the antenna is less than -10 dB which shows that there is minimum reflection loss and most of the power delivered to the antenna is radiated. Apart from this we also need to make sure that the antenna is delivering power to the specified direction which is shown by a radiation pattern plot. So, a good antenna should have a good return loss as well as an appropriate radiation pattern. And from the results above we can certainly say the modified antennas have maintained the characteristics of good antenna in the designated frequency bands.

The five different antennas of the Extreme wireless router were evaluated and after

studying their characteristics, they were modified for 3D printing. This method was helpful in learning the overall 3D printing process and the requirements that must be met for the 3D printing process. Additionally, we learned the effect of the dielectric material in the resonant frequency and the return loss. Moreover, it was a great experience to learn more about the CST Microwave Studio and deepen knowledge in antenna design.

FUTURE ENHANCEMENTS

As mentioned above, the router antennas were designed by filling a dielectric material into the antenna for 3D printing compatibility. Even though we got very good results for the blue, black, and the red wired antenna, we were not able to get such good return loss for the green and white wired antenna. In this thesis, we used a dielectric material with relative permittivity 2.45 but experimenting other dielectric material available for 3D printing could have changed the result obtained for those two antennae. Furthermore, it would be remarkable to design a general 3D printed bowtie antenna that can be made to work in a wide range of frequencies with a variation in one of the design parameters. We were able to optimize the antennas to be manufactured with the 3D printing method by comparing their performance with the originally CST simulated antennas. Due to the lack of availability of 3D printing facilities, we were actually not able to manufacture the antennas but 3D printing them and comparing the lab measurements results of these 3D printed antennas with the simulated antenna designs would be an interesting project to look into the future.

BIBLIOGRAPHY

BIBLIOGRAPHY

[1] M. Ahmadloo and P. Mousavi, "A novel integrated dielectric-and-conductive ink 3D printing technique for fabrication of microwave devices," *2013 IEEE MTT-S International Microwave Symposium Digest (MTT)*, Seattle, WA, 2013, pp. 1-3

[2] https://3dprinting.com/what-is-3d-printing/

[3] S. Moscato *et al*., "Infill-Dependent 3-D-Printed Material Based on NinjaFlex Filament for Antenna Applications," in *IEEE Antennas and Wireless Propagation Letters*, vol. 15, pp. 1506-1509, 2016.

[4] M. I. M. Ghazali, E. Gutierrez, J. C. Myers, A. Kaur, B. Wright, and P. Chahal, "Affordable 3D printed microwave antennas," *2015 IEEE 65th Electronic Components and Technology Conference (ECTC)*, San Diego, CA, 2015, pp. 240-246.

[5] O.S. Kim, "Rapid Prototyping of Electrically Small Spherical Wire Antennas," *Antennas and Propagation, IEEE Transactions*, vol. 62, no. 7, pp. 3839-3842, 2014.

[6] U. Schwarz, M. Helbig, J. Sachs, F. Seifert, R. Stephan, F. Thiel, and M.A. Hein "Physically small and adjustable double-ridged horn antenna for biomedical UWB radar applications," in *IEEE ICUWB 2008*, Hannover, Sept. 10- 12, 2008, pp 5-8.

[7] P. B. Nesbitt, H. Tsang, T. P. Ketterl, K. Church, and T. M. Weller, "4 GHz 3D-printed balun-fed bowtie antenna with finite ground plane for gain and impedance matching enhancement," *2016 IEEE 17th Annual Wireless and Microwave Technology Conference (WAMICON)*, Clearwater, FL, 2016, pp. 1-3.

[8] Xingyu Zhang and Junhong Wang, "A novel dual-band planar inverted-F antenna for WLAN applications," *2008 8th International Symposium on Antennas, Propagation, and EM Theory*, Kunming, 2008, pp. 148-151.

[9] http://www.antenna-theory.com

[10] https://www.cst.com/products/cstmws

[11] E.W Hutchcraft, "FedEx Antenna Return Loss Measurements," *BWAC Progress Report for FedEx*, Fall 2018.

VITA

Bibek Kattel

Education

Bachelor's degree in Electronics & Communications Engineering, **Tribhuvan University**, Nepal, August 2015

Academic or Professional Employment

Department of Electrical Engineering, **University of Mississippi**
Teaching Assistant (August 2017- May 2019)

In Telco Solution Pvt. Ltd , Balkumari, Lalipur, Nepal
Telecom Project Manager (May 2016 – June 2017)

Huawei Technologies Nepal Co., ltd., Lalitpur, Nepal
O & M Engineer (August 2015 – March 2016)

Mahakali Mechi Technology and Suppliers, Kathmandu, Nepal
Site Engineer (Jan 2014 - Sep 2014) & Regional Project Manager (Oct 2014 –Jul 2015)

Academic Awards

Nepal Government Scholarship Award for Deserving Engineering Student (2010)

Leadership and Professional Affiliations

Nepalese Students Association at Olemiss (NEPSA), Oxford, MS
President (April 2018-April 2019)

Nepal Engineering Council, official Engineering affiliate of Nepal Government
Registered Engineer (2015)

Student Government, Kathmandu Engineering College, Tribhuvan University
President (2012-2014)

Graduate Student Research

3D printed antenna design (May 2018 –Present)